Ionization photophysics and spectroscopy of dicyanoacetylene

Sydney Leach, Martin Schwell, Gustavo A. Garcia, Yves Bénilan, Nicolas Fray, Marie-Claire Gazeau, François Gaie-Levrel, Norbert Champion, and Jean-Claude Guillemin

Citation: The Journal of Chemical Physics **139**, 184304 (2013); doi: 10.1063/1.4826467
View online: http://dx.doi.org/10.1063/1.4826467
View Table of Contents: http://scitation.aip.org/content/aip/journal/jcp/139/18?ver=pdfcov
Published by the AIP Publishing

Ionization photophysics and spectroscopy of dicyanoacetylene

Sydney Leach,[1,a)] Martin Schwell,[2,a)] Gustavo A. Garcia,[3] Yves Bénilan,[2] Nicolas Fray,[2] Marie-Claire Gazeau,[2] François Gaie-Levrel,[3,b)] Norbert Champion,[1] and Jean-Claude Guillemin[4]

[1]*LERMA UMR CNRS 8112, Observatoire de Paris-Meudon, 5 place Jules-Jansen, 92195 Meudon, France*
[2]*LISA UMR CNRS 7583, Université Paris-Est Créteil and Université Paris Diderot, Institut Pierre Simon Laplace, 61 Avenue du Général de Gaulle, 94010 Créteil, France*
[3]*Synchrotron SOLEIL, L'Orme des Merisiers, St. Aubin, B.P. 48, 91192 Gif-sur-Yvette Cedex, France*
[4]*Institut des Sciences Chimiques de Rennes, Ecole Nationale Supérieure de Chimie de Rennes, CNRS UMR 6226, 11 Allée de Beaulieu, CS 50837, 35708 Rennes Cedex 7, France*

(Received 17 June 2013; accepted 8 October 2013; published online 11 November 2013)

Photoionization of dicyanoacetylene was studied using synchrotron radiation over the excitation range 8–25 eV, with photoelectron-photoion coincidence techniques. The absolute ionization cross-section and detailed spectroscopic aspects of the parent ion were recorded. The adiabatic ionization energy of dicyanoacetylene was measured as 11.80 ± 0.01 eV. A detailed analysis of the cation spectroscopy involves new aspects and new assignments of the vibrational components to excitation of the quasi-degenerate $A^2\Pi_g$, $B^2\Sigma_g{}^+$ states as well as the $C^2\Sigma_u{}^+$ and $D^2\Pi_u$ states of the cation. Some of the structured autoionization features observed in the 12.4–15 eV region of the total ion yield spectrum were assigned to vibrational components of valence shell transitions and to two previously unknown Rydberg series converging to the $D^2\Pi_u$ state of $C_4N_2{}^+$. The appearance energies of the fragment ions C_4N^+, C_3N^+, $C_4{}^+$, C_2N^+, and $C_2{}^+$ were measured and their heats of formation were determined and compared with existing literature values. Thermochemical calculations of the appearance potentials of these and other weaker ions were used to infer aspects of dissociative ionization pathways. © *2013 AIP Publishing LLC*. [http://dx.doi.org/10.1063/1.4826467]

I. INTRODUCTION

Dicyanoacetylene, C_4N_2, first synthesized in the early 1900s,[1] is a useful reagent for cycloaddition reactions and in the synthesis of organometallic compounds.[2] It is a particularly interesting chemical species in that it has three conjugated triple bonds (Scheme 1(a)), the central bond being a C≡C triple bond. It thus differs markedly from the related species Diacetylene, C_4H_2, which has two conjugated triple bonds (Scheme 1(b)), and a central C–C single bond.

We have previously studied aspects of the ionization photophysics and Rydberg spectroscopy of diacetylene,[3] a molecule, like dicyanoacetylene, that has considerable astrophysical interest. The presence of a centre of symmetry in linear dicyanoacetylene prevents the observation of this molecule in the interstellar medium (ISM) by rotational microwave spectroscopy. However, similar asymmetric molecules such as cyanoacetylene and cyanodiacetylene have been observed in dark clouds[4–7] in the ISM, as well as in hot circumstellar environments such as CRL 618[8,9] making it reasonable to postulate the presence of C_4N_2 in the these astrophysical sites. A possible observational target by the Herschel Space Observatory would be the strong 107 cm^{-1} infrared vibrational band of gas phase dicyanoacetylene.[10,11] An attempt to match the $C_4N_2{}^+$ cation $A^2\Pi_g \leftarrow X^2\Pi_u$ transition origin band with a diffuse interstellar band was unsuccessful.[12]

The atmosphere of Titan is mainly N_2 gas. The nitrogen atoms formed by various dissociation processes react with other ambient gases (e.g., CH_4) to synthesize a large number of hydrocarbons and nitriles.[13] Solid dicyanoacetylene has been detected in Titan's atmosphere by infrared spectroscopy (Voyager 1 IRIS spectra).[14] As the seasons change on Titan, the compound condenses and evaporates in a cycle, which allows scientists on Earth to study Titanian meteorology. Dicyanoacetylene, although not yet directly observed in the gas phase in Titan, undoubtedly exists in this phase during the evaporation stage. Complex nitrogen-bearing molecules are precursors for the production of aerosol particles, of radii 0.02–0.1 μm,[15] that are responsible for Titan's atmospheric haze. The haze structure in Titan's atmosphere is induced by a number of photochemical processes from various energy sources: solar irradiation, energetic particles existing in Saturn's magnetosphere, and galactic cosmic rays. These are capable not only of chemistry involving neutral species but also ionization processes. Thus it is of interest to investigate the VUV photophysics and photochemistry of dicyanoacetylene.

C_4N_2 was included in modelling of the photochemistry of Titan's mutually dependent atmosphere and ionosphere.[13] The stratospheric abundance of C_4N_2 was found to be highly dependent on cosmic ray dissociation of nitrogen. Alternative

a)Authors to whom correspondence should be addressed. Electronic addresses: Sydney.Leach@obspm.fr, Telephone: +33-1-4507-7561, Fax: +33-1-4507-7100 and Martin.Schwell@lisa.u-pec.fr, Telephone: +33-1-4517-1521, Fax: +33-1-4517-1564.
b)Present address: Laboratoire National de Métrologie et d'Essais (LNE), Pôle Chimie et Biologie, 1 rue Gaston Boissier, 75724 Paris Cedex 15, France.

N≡C-C≡C-C≡N 1a

H-C≡C-C≡C-H 1b

SCHEME 1. Structure of dicyanoacetylene (a) and diacetylene (b).

mechanisms for the formation of dicyanoacetylene have been proposed by Yung,[16] by Petrie and Osamura[17] and by Halpern *et al.*[18] but the relevant processes have been estimated to be only of minor importance in the overall C_4N_2 production yield in the model calculations of Lavas *et al.*,[19] although the CN addition mechanism of Halpern *et al.*,[17] in particular is considered to play a non-negligible role.[20] We note that in its flyby on 16 April 2005 the Ion and Neutral Mass Spectrometer (INMS) on board the Cassini Spacecraft recorded an ion of m/z 76 at an atmosphere altitude 1100 ± 100 km.[21] This was assigned as being essentially due to HC_5NH^+ on the basis of proton affinity properties; a possible (partial) assignment to $C_4N_2{}^+$ could not be given because of quasi-technical difficulties.

Experimental[22] and theoretical[23] studies on dicyanoacetylene anions have been carried out in the context of the increasing studies of molecular anions in the ISM[24] as well as in Titan's upper atmosphere.[25,26] Finally, we mention that a (tentative) assignment to C_4N_2 in the atmosphere of Neptune, has been reported, based on the infrared spectral measurements of Voyager 2 during its encounter on 2 August 1989.[27]

II. EXPERIMENTAL

Dicyanoacetylene was synthesized following the procedure described initially by Moureu and Bongrand[1,28] that was later modified by Miller and Lemmon.[29] It is a solid compound at ambient temperature (T_{amb}). In order to avoid its polymerisation, it must be stored at low pressure and/or diluted with a rare gas at T_{amb}. For our measurements, the gas is let into a one litre stainless steel tank to attain a pressure $p(C_4N_2) = 50$ mbar. Helium is added to yield a total pressure of $p_{TOT} \approx 3$ bars. This tank is directly connected to a molecular beam inlet using a pressure reducing regulator. The He stagnation pressure was such that no van-der-Waals aggregates were formed in the molecular beam. This was checked with the mass spectrometer.

Measurements were performed at the undulator beamline DESIRS[30] of the synchrotron radiation (SR) facility Soleil (St. Aubin, France). This beamline incorporates a 6.65 m normal incidence monochromator. For our measurements, we used the 200 grooves/mm grating which provides a constant linear dispersion of 7.2 Å/mm at the exit slit of the monochromator. The typical slit width used in our experiments is 100 μm, yielding a monochromator resolution of 0.7 Å under these conditions (about 6 meV at $h\nu = 10$ eV and 18 meV at $h\nu = 18$ eV). The beamline is equipped with a gas filter[31] which effectively removes all the high harmonics generated by the undulator that could be transmitted by the grating. In this work argon was used as a filter gas for all measurements below 15.75 eV. At higher energies, the filter is turned off. Absorption lines of the rare gas used in the filter occur in the spectra and are used to calibrate the energy scale to an absolute precision of about 1 meV. All the data were normalized with respect to the incoming photon flux, continuously measured by a photodiode (AXUV100, IRD).

The VUV output of this monochromator is directed to the permanent end station SAPHIRS which consists of a molecular beam inlet and an electron-ion coincidence spectrometer called DELICIOUS II. The latter has been described recently in detail.[32] A brief description is given here: The monochromatised SR beam (200 μm horizontal × 100 μm vertical extensions) is crossed at a right angle with the molecular beam at the centre of DELICOUS II which combines a photoelectron velocity map imaging (VMI) spectrometer with a linear time-of-flight mass analyzer operating according to Wiley-MacLaren space focusing conditions. The spectrometer is capable of photoelectron/photoion coincidence (PEPICO) measurements where photoelectron images can be recorded for a chosen ion mass. The electron images can be treated to obtain the threshold photoelectron spectroscopy of the selected cation, and reveal its electronic structure via the Slow Photoelectron Spectroscopy (SPES) method, which has been described in Refs. 33 and 34 and will also be explained in Sec. IV B. In addition, total ion yields (TIY) as a function of photon energy can be acquired where the spectral resolution is defined only by the slit widths of the monochromator (see above).

For half of the experimental campaign, C_4N_2 was further mixed with propane (C_3H_8) as a standard at equal pressure $p(C_4N_2) = p(C_3H_8) = 50$ mbar, in order to measure absolute ionization cross-sections according to the comparative method described by Cool *et al.*[35] and using the cross-section data given by Kameta *et al.*[36] Also here, helium was added to yield a total pressure of $p_{TOT} = 3$ bar. The pressure was measured with a Baratron (MKS). The absolute error of this pressure transducer is estimated to be about ±3%. The relative yield of m/z 76 ($C_4N_2{}^+$) as compared to m/z 44 (propane $C_3H_8{}^+$) has been further multiplied by a factor of 1.356 in order to take into account the convoluted mass transmission function of SAPHIRS and DELICOUS II, calibrated with known gases with mass ranges between m/z 18 and 142. For absolute measurements, the extraction field was set so that all the electrons and ions were collected.

III. ELECTRONIC, VIBRATIONAL, AND GEOMETRIC STRUCTURAL PRELIMINARIES

In order to interpret the results of our experiments that are described in Sec. IV it is useful to present here information on the electronic, vibrational, and geometrical structures of neutral and ionic diacyanocetylene.

A. Electronic structure

Experimental HeI and HeII photoelectron spectra of dicyanoacetylene and assignments reported by Bieri *et al.*[37] and Asbrink *et al.*[38] have provided the following successive ionization energies and assigned molecular orbital (M.O.) symmetries corresponding to the ejected electrons: 11.84 eV $2\pi_u$,

13.91 eV $4\sigma_g$, 14.00 eV $3\sigma_u$, 14.16 eV $1\pi_g$, 15.00 eV $1\pi_u$, 20.7 eV $3\sigma_g$, 23.0 eV $2\sigma_u$, thus giving the electron configuration corresponding to the ground state of the dicyanoacetylene ion as ... $2\sigma_u^2\ 3\sigma_g^2\ 1\pi_u^4\ 1\pi_g^4\ 3\sigma_u^2\ 4\sigma_g^2\ 1\pi_u^3\ X^2\Pi_u$ ($=1^2\Pi_u$). The M.O. assignments were mainly based on calculations both in Koopmans' approximation and by an *ab initio* many-body Green's function method.

The order of the M.O.s has been revised more recently. It has been shown that the $4\sigma_g$, $3\sigma_u$, and $1\pi_g$ M.O.s are quasi degenerate,[39] so that the resulting $1^2\Sigma_g^+$, $1^2\Sigma_u^+$, and $1^2\Pi_g$ electronic states of the ion are likely to be vibronically coupled. Based on their interpretation of emission and excitation spectra of the dicyanoacetylene ion Maier *et al.*[39] revised the order of the M.O.s so that the $1\pi_g$ orbital became the lowest lying of the three quasi-degenerate M.O.s and thus the $1^2\Pi_g$ electronic state was predicted to lie below the $1^2\Sigma_g^+$ and $1^2\Sigma_u^+$ states. An *ab initio* calculation study by Cao and Peyerimhoff[40] also predicted this order of the electronic states, with the $1^2\Sigma_g^+$ and $1^2\Sigma_u^+$ states computed to lie, respectively, 80 meV and 130 meV above the $1^2\Pi_g$ state. However, further experimental work by the Maier group[41] showed that the $1^2\Pi_g$ and $1^2\Sigma_g^+$ states are intimately mixed (see below).

B. Geometry

The geometrical structure of neutral dicyanoacetylene has been determined by electron diffraction and coherent Raman spectroscopy.[42] As expected from its electronic structure it is a linear molecule; its bond lengths are r(N≡C) = 1.161 Å; r(C≡C) = 1.198 Å; r(C–C) = 1.367 Å. There are no direct determinations of the bond lengths in the ion but we can compare calculated values of both neutral and ion ground state bond lengths. Table I gives the relevant data. The calculated internuclear distances of neutral dicyanoacetylene ground state in Table I are in good agreement with experiment. Although the calculated bondlengths of the ground state of the ion differ by 1%–4% in the various calculations, these ion state values in Table I are sufficiently different from those of the neutral molecule to allow us a valid comparison between the ion and neutral bondlengths. This shows that in going from the neutral to the ion ground state r(N≡C) increases by about 2%–4%, r(C≡C) increases by about 2%–4% and r(C–C) decreases by about 3%, whereas in going to the $1^2\Pi_g$ excited state of the ion r(N≡C) increases by 3%–4%, r(C≡C) remains unchanged and r(C–C) decreases about by 2%–3%.

This comparison of ground state neutral and ion corresponding bondlengths indicates that on ionization CN and CC stretching vibrations are likely to be excited and, furthermore, that the N≡C and C≡C bonds should acquire some measure of double bond character, thus increasing the tendency to linear structure as exemplified in cumulenes.

TABLE I. Dicyanoacetylene: neutral molecule and cation bondlengths.

Species	r(N≡C) (Å)	r(C≡C) (Å)	R(C–C) (Å)	Method
NCCCCN	1.161	1.198	1.367	Expt.[42]
NCCCCN	1.156	1.210	1.363	Calc.[a]
NCCCCN	1.161	1.210	1.383	Calc.[b]
NCCCCN	1.159	1.210	1.363	Calc.[c]
$NCCCCN^+\ X^2\Pi_u$	1.1922	1.2504	1.3383	Calc.[d]
$NCCCCN^+\ X^2\Pi_u$	1.1806	1.2273	1.3308	Calc.[e]
$NCCCCN^+\ X^2\Pi_u$	1.177	1.239	1.335	Calc.[f]
$NCCCCN^+\ X^2\Pi_u$	1.199	1.258	1.349	Calc.[g]
$NCCCCN^+\ X^2\Pi_u$	1.175	1.229	1.347	Calc.[h]
$NCCCCN^+\ A^2\Pi_g$	1.206	1.209	1.344	Calc.[h]

[a]Density Functional Theory (DFT) method.[4]
[b]CASSCF.[43]
[c]DFT (B3LYP).[44]
[d]Density Functional Theory (DFT) method.[45]
[e]CASSCF.[46]
[f]Density Functional Theory (DFT) method B3LYP.[40]
[g]Density Functional Theory (DFT) method B3LYP.[47]
[h]CASSCF.[47]

C. Vibrations

The frequencies of dicyanoacetylene ground state vibrations are well known from IR and Raman studies.[48] Corresponding data for the cation electronic states is known from a variety of optical spectroscopy and photoelectron spectroscopy studies as well as some theoretical calculations. These values, the corresponding references previous to the present study are listed in Table II. Vibrational aspects of the ion electronic states as exhibited in the PEPICO (TIY) and SPES spectra will be discussed below. The vibrational frequencies resulting from our analysis of the SPES spectra, presented below, are also given in Table II.

IV. RESULTS AND DISCUSSION

A. The photoion mass spectra

Photoion mass spectra were observed at selected photon excitation energies between 12 and 20 eV (Figs. 1(a) and 1(b)). An additional mass spectrum was measured at $E_{exc} = 25$ eV but is not shown here. These spectra were obtained with an extraction field such that ions with coincident electrons having more than 0.95 eV kinetic energy will be discriminated, so that for instance the parent ion count will appear to be lower for $h\nu > 12.8$ eV since it correlates to the fastest electrons. At $E_{exc} = 12$ eV the only ions present are the parent ion m/z 76 and the $^{13}CC_3N_2^+$ carbon isotopic ion at m/z 77 (5% relative intensity). At $E_{exc} = 16$ and 17 eV these ions are accompanied by impurity ions m/z 40 (Ar^+), m/z 32 (O_2^+), m/z 28 (N_2^+), and m/z 18 (H_2O^+) (not shown). On increasing the excitation energy to $E_{exc} = 18$ eV a very weak signal appears at m/z 48, assigned to the C_4^+ ion (Fig. 1(c)). This fragment ion is clearly visible at $E_{exc} = 18.5$ eV (Fig. 1(d)). Three new fragment ions, C_2N^+ (m/z 38), C_3N^+ (m/z 50), and C_4N^+ (m/z 62) are observed at $E_{exc} = 19$ eV (Fig. 1(e)). The same set of ions is found at $E_{exc} = 20$ eV with some changes in their relative signal intensities (Fig. 1(f)). More details on the excitation energy dependence of the parent and fragment ion intensities are discussed below.

TABLE II. Vibrational frequencies (cm^{-1}) in neutral and ionic dicyanoacetylene. Present study values are in bold italics.

Vibration	Neutral $X^1\Sigma_g^+$[48]	Ion $X^2\Pi_u$	Ion $A^2\Pi_g$, $B^2\Sigma_g^+$	Ion $C^2\Sigma_u^+$	Ion $D^2\Pi_u$
ν_1(C≡N)	2297[a]	2210[39,49] 2220[b,50] ***2184***	2151[39] 2200[51] 2154[b,50] ***2186***[c]	***2056***	***2033***
ν_2(C≡C)	2123	1930[39,49] 1942[b,50] ***1972***	2099[39] 2094[b,50] ***2008***	***1774***	2100[c,51] ***1750***
ν_3(C–C)	620	570[39,49] 613[b,50] ***575***	696[39] 511[b,50] ***625***		590[51] ***563***
ν_4	2245	2010[b,50] 2015[b,52]			
ν_5	1155	1208[b,50]			
ν_6	505	568 calc.[40] 558 calc.[53]			
ν_7	261	266 calc.[40] 266 calc.[53] ***258***			
ν_8	472	477 calc.[40] 459 calc.[53]			
ν_9	107	108 calc.[40] 113 calc.[53]			

[a]Corrected for Fermi resonance. ν_1(C≡N) is assigned (C≡C) by Khanna *et al.*[10] at 2331 cm^{-1} but Winther and Schönhoff[48] show that it is $2\nu_5$ in Fermi resonance with ν_1 at 2268 cm^{-1}.
[b]Ne matrix values.
[c]PES band frequency assigned by Baker and Turner[51] to ν_2(C≡C) by similarity with neutral ground state frequency. We consider that an assignment to ν_1(C≡N) is also possible.

B. Slow photoelectron spectroscopy (SPES) of the dicyanoacetylene parent cation: Analysis and assignments

As mentioned in Sec. II, the spectrometer records mass-selected photoelectron images. These images are then Abel inverted using the pBasex algorithm[54] to yield photoelectron spectra at any and all the photon energies of the scan. The data are displayed in the form of an intensity matrix in Fig. 2(a) for the $C_4N_2^+$ parent ion over the 11.5–15.5 eV photon excitation energy region. In such a matrix, the number of e^-/i^+ coincidences (given in a color code) are plotted as a function of electron kinetic energy and photon energy. It carries a wealth of information that can be reduced in different ways. By energy conservation, electrons ejected into the continuum through a direct process will appear as diagonal lines of constant slope ($h\nu - IE_i/KE$ where $h\nu$ is the photon energy, IE_i is the ionization energy of the ith state, and KE is the electron kinetic energy. As described in Ref. 33, one can now integrate the electron signal along the slope direction up to a certain KE for each photon energy to obtain the SPES, which provides the cation spectroscopy with high electron resolution without compromising the signal to noise ratio. The integration range chosen here ($0 < KE < 50$ meV) yields an electron resolution of ≈25 meV.

The resulting SPES for the m/z = 76 ion are shown in Fig. 2(b) over the range 11.5–15.5 eV. The same 11.5–15.5 eV bands have previously been observed by a technique analogous to that of SPES, in a photoelectron spectrum recorded with a constant halfwidth band pass of 25 meV.[49] Three spectral regions can be seen between 11.8 and 15.5 eV with the band positions compiled in Table III. Graphical zooms of the regions of interest are given in Fig. 3 which includes band assignments that are presented below. The non-assigned features in Table III and Fig. 3 are very weak and are probably mainly noise produced.

1. $X^2\Pi_u$ ion state region 11.8–13.8 eV

In the first region (Fig. 3(a)) there is a strong SPES band peaking at 11.835 eV, FWHM = 155 cm^{-1}, which can be considered as the vertical ionization energy IE_v of dicyanoacetylene and is thus the origin band of the $X^2\Pi_u$ ion state and is the first of an apparent progression of 4 bands. The interval of 275 meV (2218 cm^{-1}) between the first two bands in this progression is typical of the successive progression intervals and it can be assigned to the ν_1(C≡N) stretching vibration whose 2210 ± 10 cm^{-1} ion ground state frequency is best known experimentally from the emission spectra of Maier *et al.*[49] (Table II). The ν_2(C≡C) vibration, whose frequency is 1942 cm^{-1}, as observed in emission spectra[39,49] (Table II), is expected to be excited at 12.076 eV and is indeed present at that energy as a shoulder on a strong band (Fig. 3(a)). The changes in the C≡C bondlength on ionization (Table I) make it likely, Franck-Condon-wise, that the ν_2(C≡C)

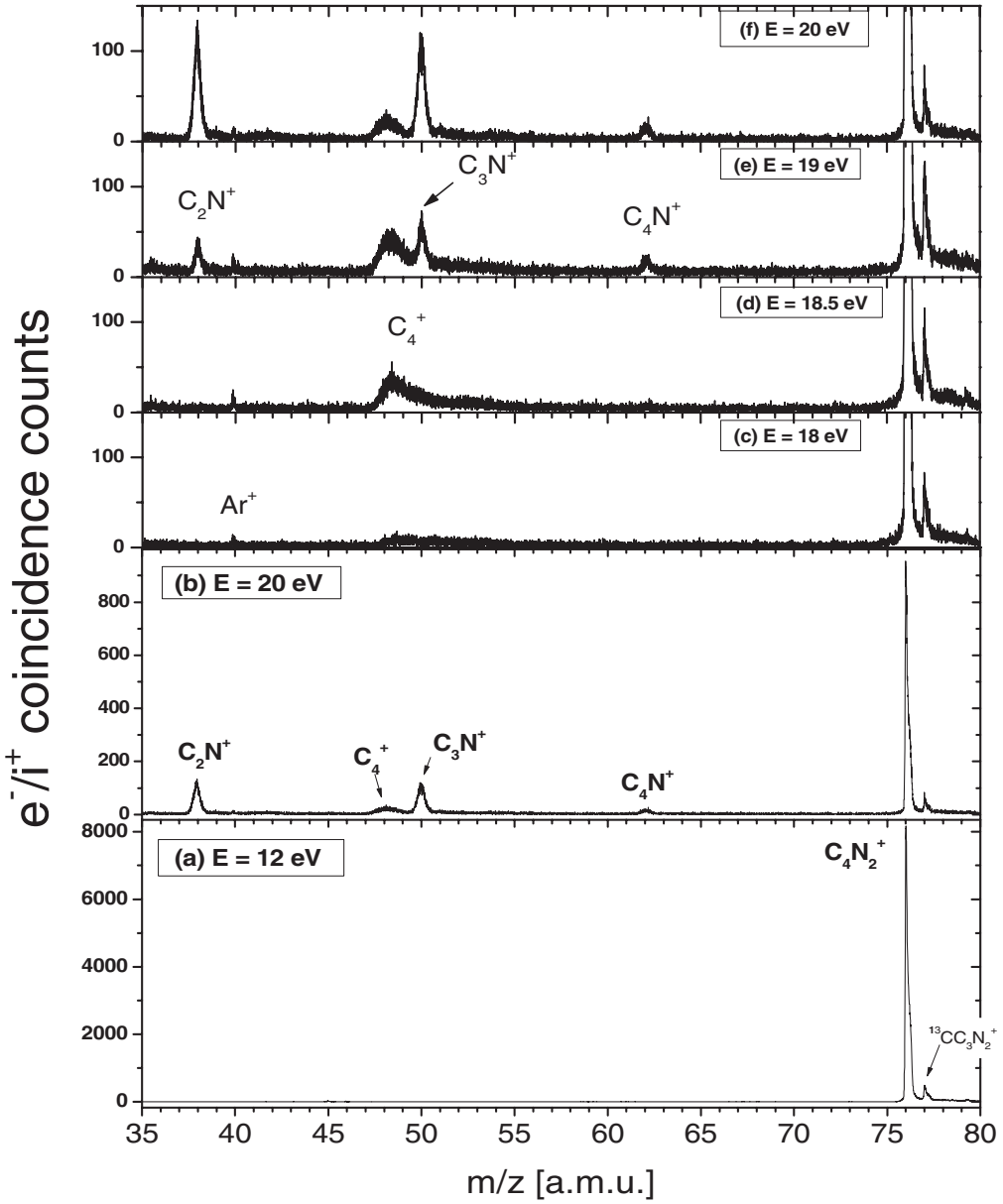

FIG. 1. Photoion mass spectra of dicyanoacetylene at (a) E = 12 eV and (b) E = 20 eV, recorded with an extraction field of 95 V/cm (electron KE_{max} = 0.95 eV) and no propane in the sample. A vertical zoom of the intermediate photon energies is shown in panels (c)–(f).

will be excited; there are, indeed, some ragged features also in the region where excitation of $2\nu_2$(C≡C) should occur.

In this first region there are also some other weak, not well-defined broad features. Band intervals of ≈570 cm^{-1} and ≈1090 cm^{-1} can be recognised. These can reasonably be considered as vibrational intervals of a progression of the ν_3(C–C) stretch vibration whose ion ground state value is known to be 570 ± 10 cm^{-1} in the gas phase (Table II). Excitation of the bending frequency ν_7 also appears to occur. The SPES in the $X^2\Pi_u$ ion state region are very similar to that of HeI PES[39] but a little better resolved and so more amenable to analysis. The geometrical changes on ionization of dicyanoacetylene discussed above indicate that on ionization to the $X^2\Pi_u$ ion ground state one would expect to excite progressions in NC and CC stretching vibrations as are indeed revealed by the SPES.

2. The ion triple state region 13.8–14.4 eV

In the second SPES region, between 13.8 and 14.4 eV (Fig. 3(b)) the bands observed are essentially those observed in this region in HeI PES by Baker and Turner[51] and by Maier *et al.*[39] and which arise by electron ejection from quasi-degenerate $4\sigma_g$, $3\sigma_u$, and $1\pi_g$ M.O.s. The resulting $1^2\Sigma_g^+$, $1^2\Sigma_u^+$, and $1^2\Pi_g$ electronic states of the ion will be close-lying and subject to vibronic coupling. This is of great interest and a source of problems for spectral analysis involving these states. As mentioned above, in the revised the order of the molecular orbitals by Maier *et al.*[39] the $1\pi_g$ orbital became the

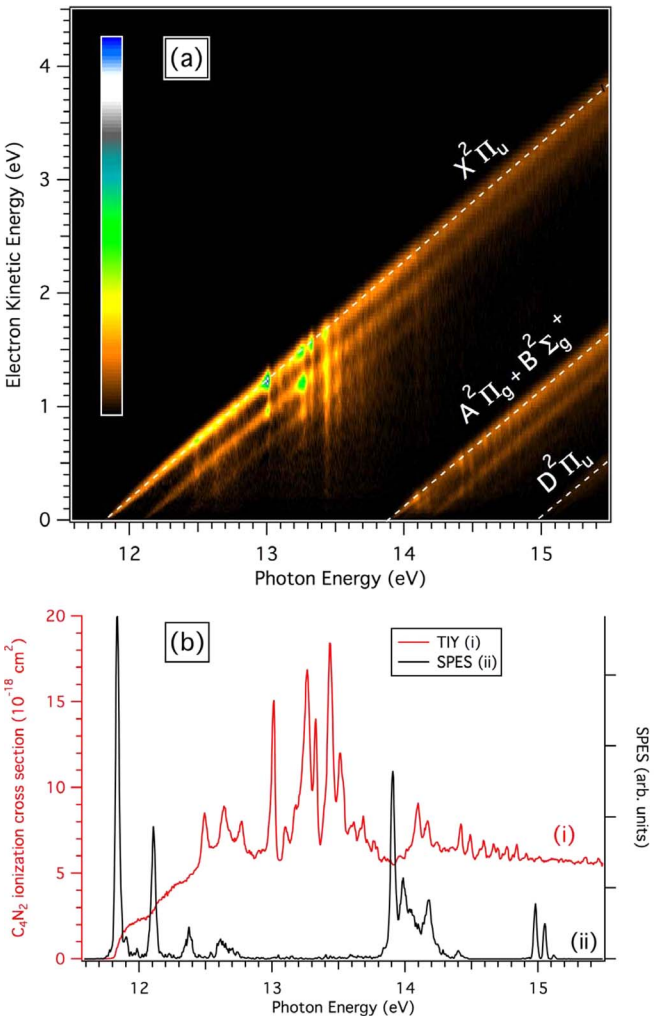

FIG. 2. (a) Photoelectron intensity matrix of dicyanoacetylene obtained with an extraction field of 572 V/cm (electron $KE_{max} = 5.7$ eV). The color code gives the number of e^-/i^+ coincidences (increasing from black to blue) as a function of photon energy and electron kinetic energy. The white diagonal dashed lines trace the electronic states of the cation (see our detailed explanation in Sec. IV B). (b) Derived slow photoelectron spectrum (SPES; black curve) and total ion yield (TIY; red curve). Note that the ordinate of the TIY spectrum is given in absolute ionization cross sections (see text for details).

TABLE III. Dicyanoacetylene: Vibronic transitions to cation states in the SPES spectrum.

SPES band no.	E (eV)	E (cm^{-1})	Assignment
1	11.835	95 455	$X^2\Pi_u\ O^0_0$
2	11.867	95 713	$X^2\Pi_u\ 7^1_0$
3	11.903	96 004	$X^2\Pi_u\ 3^1_0$
4	11.984	96 657	$X^2\Pi_u\ 3^2_0$
5	12.076 sh[a]	97 399	$X^2\Pi_u\ 2^1_0$
6	12.107	97 649	$X^2\Pi_u\ 1^1_0$
7	12.331	99 456	$X^2\Pi_u\ 2^2_0$
8	12.374 max	99 802	$X^2\Pi_u\ 1^2_0$
9	12.390 sh	99 932	
10	12.541	101 149	
11	12.613 broad	101 730	$X^2\Pi_u\ 1^3_0$
12	12.651	102 037	
13	12.691	102 359	
14	12.741	102 763	
15	13.907	112 167	$A^2\Pi_g, B^2\Sigma_g^+\ O^0_0$
16	13.965	112 635	
17	13.984	112 788	$A^2\Pi_g, B^2\Sigma_g^+\ 3^1_0$
18	13.995	112 877	
19	14.006	112 965	
20	14.034	113 191	
21	14.047	113 296	
22	14.063	113 425	$A^2\Pi_g, B^2\Sigma_g^+\ 3^2_0$
23	14.100	113 724	
24	14.136	114 014	
25	14.156	114 175	$A^2\Pi_g, B^2\Sigma_g^+\ 2^1_0$
26	14.178	114 353	$C^2\Sigma_u^+\ O^0_0$; $A^2\Pi_g, B^2\Sigma_g^+\ 1^1_0$
27	14.201	114 538	
28	14.217	114 667	
29	14.241	114 861	
30	14.285	115 216	
31	14.378	115 966	
32	14.398	116 127	$C^2\Sigma_u^+\ 2^1_0$
33	14.433	116 409	$C^2\Sigma_u^+\ 1^1_0$; $A^2\Pi_g, B^2\Sigma_g^+\ 1^2_0$
34	14.979	120 813	$D^2\Pi_u\ O^0_0$
35	15.049	121 378	$D^2\Pi_u\ 3^1_0$
36	15.118	121 934	$D^2\Pi_u\ 3^2_0$
37	15.196	122 563	$D^2\Pi_u\ 2^1_0$
38	15.231	122 846	$D^2\Pi_u\ 1^1_0$

[a]sh = shoulder.

lowest lying of the three quasi-degenerate M.O.s and thus the $1^2\Pi_g$ electronic state was predicted to lie below the $1^2\Sigma_g^+$ and $1^2\Sigma_u^+$ states. However, further work by this group,[41] who analysed perturbation features in a rotationally resolved $A^2\Pi_g \leftarrow X^2\Pi_u$ ($1^2\Pi_g \leftarrow 1^2\Pi_u$) absorption transition of the dicyanoacetylene cation, showed that the $1^2\Sigma_g^+$ electronic state lies about 208 cm^{-1} (26 meV) below the $1^2\Pi_g$, $\Omega = \frac{1}{2}$ state, the $1^2\Pi_g$ state, like the $1^2\Pi_u$ doublet state, being a spin-orbit inverted state ($A_0(1^2\Pi_g) \approx -40$ cm^{-1}).

The $1^2\Pi_g$ and $1^2\Sigma_g^+$ ion states are thus intimately mixed. We have therefore assigned the SPES band at 13.907 eV (Fig. 3(b) and Table III) to joint origin bands of the $A^2\Pi_g$ and $B^2\Sigma_g^+$ electronic states, assuming that each succeeding vibronic band has characteristics of each of the two electronic states. A progression in ν_3(C–C) is assigned. A possible vibrational progression in ν_1(C≡N) would overlap bands involving the $C^2\Sigma_u^+$ state (Table III). These vibrational assignments are compatible with the results of gas phase fluorescence excitation spectra which delineated ν_1, ν_2, and ν_3 vibrational frequencies in the $A^2\Pi_g$ state.

We note that the $A^2\Pi_g$ state bondlength calculations of Zhao *et al.*[47] (Table I), which neglect effects of vibronic interactions, indicate that on ionization to this state we should expect progressions in NC and CC stretching vibrations.

In contrast to our detailed knowledge of the $A^2\Pi_g$ and $B^2\Sigma_g^+$ ion state energies[41] that of $C^2\Sigma_u^+$, the third member of the triplet of states in the 14 eV region, is less well assured. Nagarajan and Maier[55] place the $C^2\Sigma_u^+$ state origin as 18 720 cm^{-1} above the ionization energy of dicyanoacetylene, which is compatible with our assignment of the $C^2\Sigma_u^+\ O^0_0$ origin to the strong SPES feature at 14.178 eV (Fig. 3(b)). However, we stress that there is no independent assignment of this transition energy; the assignments based on HeI photoelectron spectra depend largely on calculations, in particular Green's function calculations,[39] which are very sensitive to the choice of geometries.

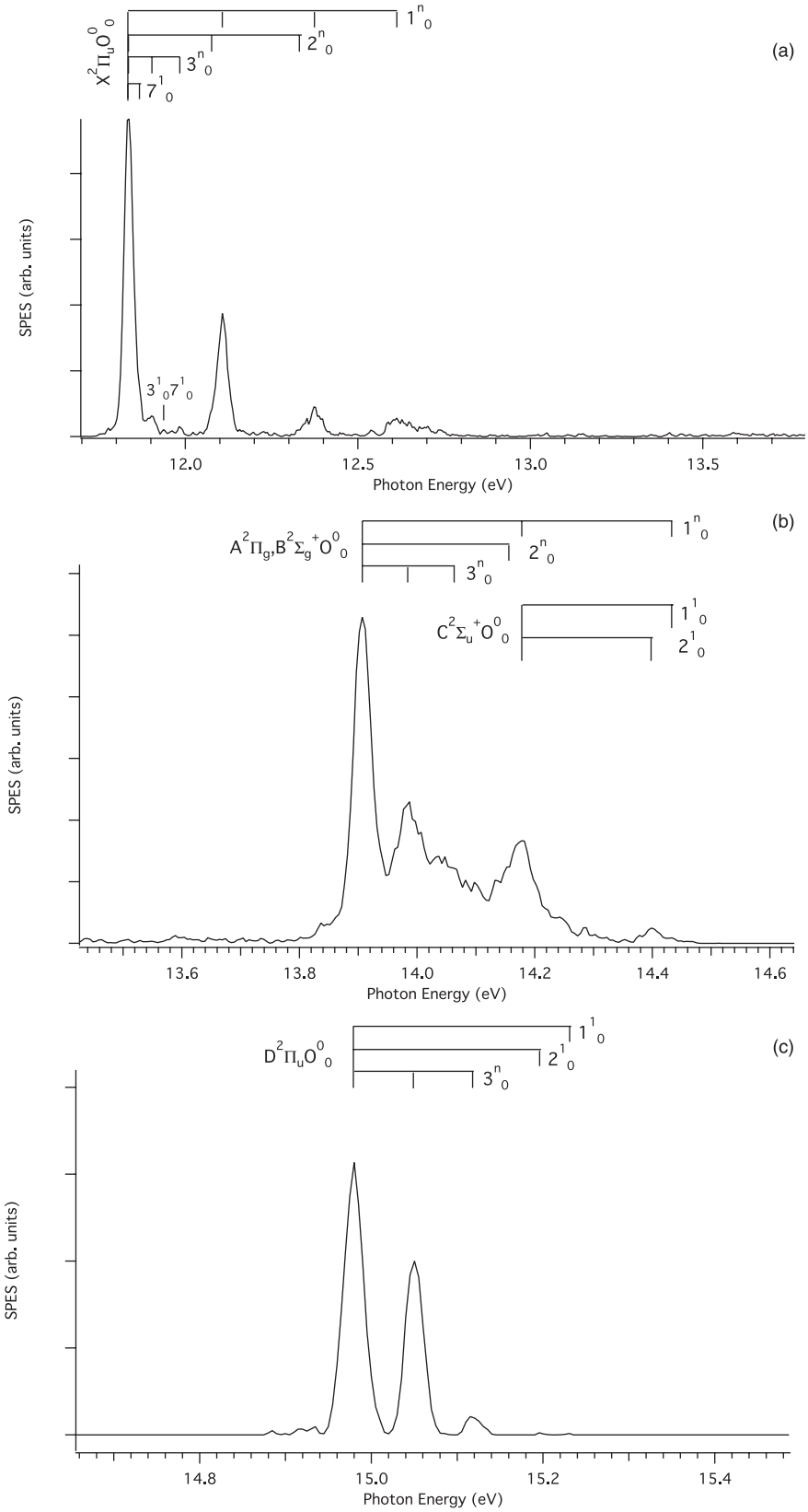

FIG. 3. Slow photoelectron spectra (SPES) of dicyanoacetylene: (a) 11.7–13.8 eV, (b) 13.5–14.6 eV, and (c) 14.7–15.4 eV.

Absorption spectra and fluorescence excitation spectra in the gas phase[39] and in the rare gas matrix phase,[50,52] purporting to be of the $A^2\Pi_g \leftarrow X^2\Pi_u$ transition of the dicyanoacetylene ion should, in principle, be of help in disentangling the vibronic interactions, which is certainly the case for the $A^2\Pi_g$, $B^2\Sigma_g^+$ states[41] discussed above. However, the $C^2\Sigma_u^+ \leftrightarrow X^2\Pi_u$ transition is electric dipole forbidden and would only be observable as weak Herzberg-Teller vibronic

transitions involving excitation of ungerade vibrations (σ_u^+: ν_4, ν_5; π_u: ν_8, ν_9). Maier *et al.* mention that there are unidentified broad bands around 19 000 cm^{-1} in the gas phase fluorescence excitation spectrum.[39] These could perhaps be related to excitation to the $C^2\Sigma_u^+$ state. Sharp bands in the 18 750–18 900 cm^{-1} region, where forbidden $C^2\Sigma_u^+ \leftrightarrow X^2\Pi_u$ transition features could occur, were observed by Agreiter *et al.*[50] in the Ne matrix fluorescence excitation spectrum but were assigned to vibrational components of the $A^2\Pi_g \leftarrow X^2\Pi_u$ transition.

Our SPES assignments in the 14.178 to 14.433 eV region (Table III) include possible overlapping vibronic assignments to the triplet of states $A^2\Pi_g$, $B^2\Sigma_g^+$ and $C^2\Sigma_u^+$, e.g., SPES bands at 14.178 and 14.333 eV. Because of the vibronic entanglement of the three states, including possible Renner-Teller effects in the $A^2\Pi_g$ state, it is expected that the observed SPES vibrational intervals associated with these states will be irregular. Thus the $A^2\Pi_g$, $B^2\Sigma_g^+$, and $C^2\Sigma_u^+$ state vibrational frequencies resulting from our SPES analysis, and which are gathered together and reported in Table II, are average effective values. They are also subject to uncertainty (2–10 meV) in determining and measuring the energies of peak or shoulder features in the SPES. We note that the values of the $C^2\Sigma_u^+$ and $D^2\Pi_u$ state carbon-carbon vibrational frequency, respectively, ν_2 = 1774 and 1750 cm^{-1} (Table II) signal a strong tendency for cumulene structure of dicyanoacetylene in these electronic states. Much higher spectral resolution and accompanying theoretical computations of the vibronic interactions are necessary for further progress in elucidating the vibrational structures under study.

3. $D^2\Pi_u$ ion state region 14.9–15.2 eV

The third SPES region, between 14.9 and 15.2 eV contains three prominent bands, forming a progression and two very weak features (Fig. 3(c)). Bands in this region were assigned by Maier *et al.*[49] to the electronic state $D^2\Pi_u$, with vibrational features. The $D^2\Pi_u$ state origin band at 14.979 ± 0.005 eV is followed by a progression of the prominent bands whose successive intervals are ≈ 560 cm^{-1}. This is undoubtedly the ν_3(C–C) stretch vibration, given as 590 cm^{-1} by Baker and Turner[51] (Table II). The weak features include a band corresponding to excitation of the ν_2(C≡C) vibration. The $D^2\Pi_u$ state origin band is intermediate in energy between the previously reported PES values 14.95 ± 0.01 eV[51] and 15.0 eV.[37–39,49] As shown below (Sec. IV C 3) the variation of the quantum defect over the n = 3–9 members of the Rydberg series converging to the $D^2\Pi_u$ state of the ion is small (Table IV). This confirms our 14.979 ± 0.005 eV value for the $D^2\Pi_u$ state origin band.

It is of interest that the $C^2\Sigma_u^+$ and $D^2\Pi_u$ states once formed are not isolated states since they rapidly relax by internal conversion to high vibrational levels of the $A^2\Pi_g$ state from which Franck-Condon modulated fluorescence occurs to suitable vibrational levels of the $X^2\Pi_u$ ground state of the ion.[39]

TABLE IV. Dicyanoacetylene: Valence shell and Rydberg transitions in the TIY m/z = 76 spectrum. δ = quantum defect.

Band No.	eV	cm^{-1}	Assignment
1	12.492	100 754	V1 O^0_0
2	12.634	101 896	V1 5^1_0
3	12.677	102 246	
4	12.766	102 964	V1 5^2_0
5	13.009	104 924	V2 O^0_0
6	13.097	105 634	V2 3^1_0
7	13.174	106 255	V2 3^2_0
8	13.209 sh[a]	106 537	
9	13.260	106 949	V2 2^1_0; R1 (n = 3, δ = 0.18) O^0_0
10	13.324	107 465	R1 (n = 3) 3^1_0
11	13.393 sh	108 021	R1 (n = 3) 3^2_0
12	13.432	108 336	R2 (n = 4, δ = 1.03) O^0_0
13	13.509	108 957	V2 2^2_0; R1 (n = 4) 3^2_0
14	13.530 sh	109 126	
15	13.601	109 699	
16	13.652 sh	110 110	
17	13.682	110 352	R2 (n = 4) 1^1_0
18	13.760	110 981	V2 2^3_0
19	13.948	112 498	R2 (n = 4) 1^2_0
20	14.030	113 159	
21	14.092	113 659	R1 (n = 4, δ = 0.08) O^0_0
22	14.162	114 224	R1 (n = 4) 3^1_0; R2 (n = 5, δ = 0.92) O^0_0
23	14.231	114 780	R1 (n = 4) 3^2_0
24	14.346	115 708	
25	14.412	116 240	R1 (n = 5, δ = 0.10) O^0_0
26	14.482	116 805	R1 (n = 5) 3^1_0
27	14.557	117 409	R1 (n = 5) 3^2_0
28	14.585	117 635	R1 (n = 6, δ = 0.12) O^0_0
29	14.660	118 240	R1 (n = 6) 3^1_0
30	14.689	118 474	R1 (n = 7, δ = 0.15) O^0_0
31	14.734	118 837	R1 (n = 6) 3^2_0
32	14.758	119 031	R1 (n = 8, δ = 0.15) O^0_0; R1 (n = 7) 3^1_0
33	14.804	119 402	R1 (n = 9, δ = 0.18) O^0_0
34	14.832	119 628	R1 (n = 8) 3^1_0; R1 (n = 7) 3^2_0
35	14.901	120 184	R1 (n = 8) 3^2_0
36	15.007	121 039	

[a]sh = shoulder.

C. TIY spectra of the dicyanoacetylene parent cation: Analysis and assignments

Integration of all the photoelectron kinetic energies as a function of the photon energy, performed on the photoelectron matrix in Fig. 2(a), gives the Total Ion Yield (TIY) spectrum of the parent ion plotted in Fig. 2(b) between 11.6 and 15.4 eV and presented in more detail in Fig. 4 for the region 12.2–15.2 eV. We discuss below the analysis of this spectrum.

1. Ionization energy

From the TIY spectrum of the parent ion $C_4N_2^+$ at m/z = 76 (Fig. 2(b)) we measure an ionization energy IE (C_4N_2) = 11.80 ± 0.01 eV. This is greater than the electron impact value reported by Dibeler *et al.*,[56] IE (C_4N_2) = 11.4 ± 0.2 eV. The latter value must be rejected since it is close to that of acetylene IE(C_2H_2) = 11.40 ± 0.002 eV[57] and would thus imply, incorrectly, that the ejected electron is localised on the

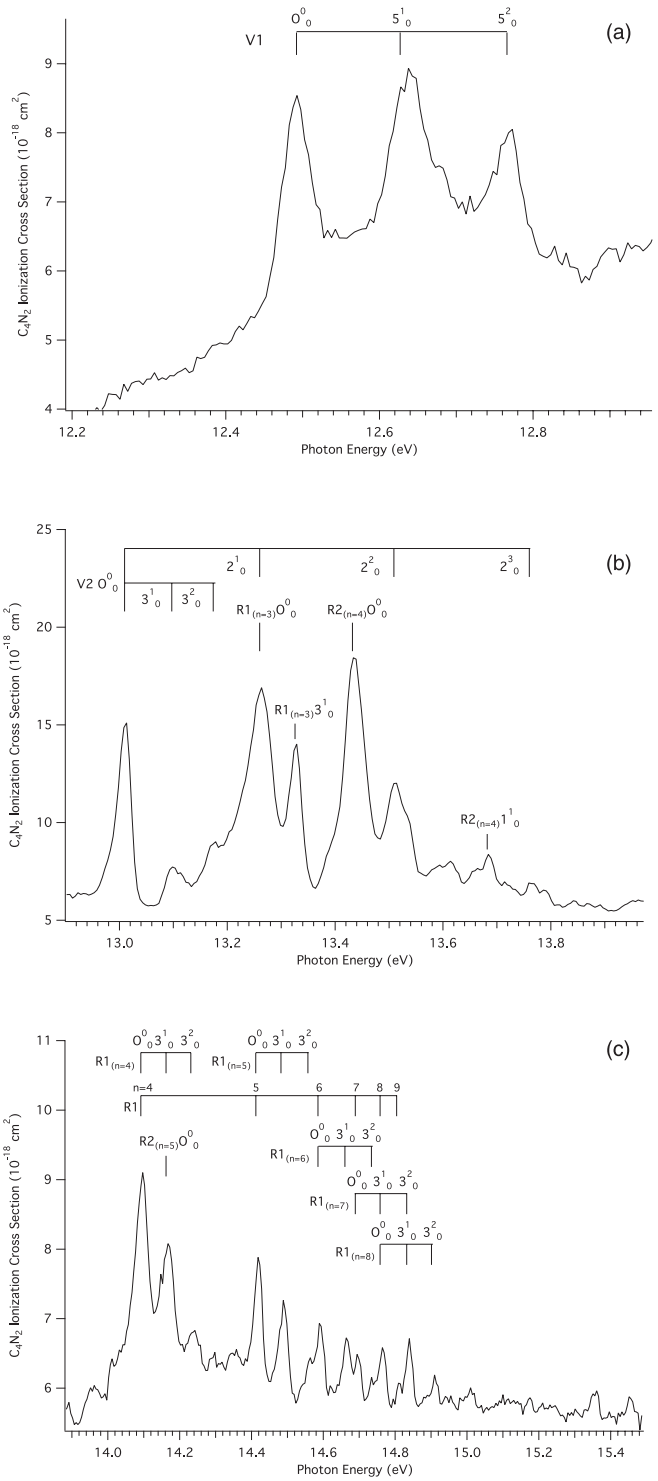

FIG. 4. Total Ion yield spectra (TIY) of the dicyanoacetylene ion, m/z 76: (a) 12.2–12.9 eV, (b) 12.9–13.9 eV, and (c) 13.9–15.4 eV.

C≡C bond. Our IE_{ad} (C_4N_2) = 11.80 ± 0.01 eV and IE_{vert} = 11.835 eV (Sec. IV B) values agree well with reported PES values IE (C_4N_2) = 11.84 eV of Bieri *et al.*[37] and IE (C_4N_2) = 11.81 eV.[51]

Since the heat of formation of C_4N_2 is 533.46 kJ/mol (5.528 eV),[57] our ionization energy therefore leads to a value of the heat of formation of the dicyanoacetylene ion $\Delta_f H(C_4N_2^+)$ = 1672 kJ/mol (17.328 eV).

2. Autoionisation structures

A series of bands are observed in the TIY spectrum of the parent ion between 12.5 eV and 14 eV, and a second series between 14 and 15 eV (Figs. 2(b) and 4, and Table IV). These bands must be autoionization features since, as seen in Fig. 2(a), they occur at fixed photon energies and their electron kinetic energies do not follow lines of constant slope as in direct ionization. We divide the bands into three groups. Band assignments are given in Table IV and in Fig. 4. The first group, between 12.49 and 12.95 eV (Fig. 4(a)), has 3 main peaks (Bands 1, 2, and 4, Table IV), forming a progression, based on Band No. 1 as the O^0_0 origin, in a vibration of frequency $\nu \approx 1150 \pm 50$ cm^{-1} that we suggest is the ν_5 (C–C) antisymmetric stretching vibration, of vibrational symmetry σ_u^+. This progression is designated as belonging to the V1 transition, probably a valence-shell transition, as discussed in Sec. IV C 4.

The second region (Fig. 4(b) and Table IV) begins at 13.009 eV and goes up to 14 eV. Its first band (Band No. 5) is the origin of a progression of four features whose successive intervals are 2025, 2008, and 2024 cm^{-1}, assignable to excitation of the ν_2 (C≡C) symmetric stretch vibration but which overlap Rydberg bands, as discussed below. Another progression, Band Nos. 5, 6, and 7, intervals 710, 621 cm^{-1}, could correspond to the σ_g^+ ν_3 (C–C) symmetric stretch vibration (whose value is 690 cm^{-1} in the $A^2\Pi_g$ ion state). These two progressions are considered to be members of another valence-shell transition, V2.

It is of interest to analyse the relaxation pathways by measuring the electron kinetic energy. Figure 5 displays KE projections for the photon energies corresponding to VI and V2 transition bands as well as some Rydberg bands to be discussed later. We first discuss the valence-shell transition electron K.E. spectra. The spectra at specific band excitation energies will contain two components, a background component due to direct ionization and a resonance component due to autoionization. In the latter case the ionizing transition is indirect, in that it now occurs from a superexcited neutral state lying above the ionization energy, instead of directly from the neutral ground state in the case of direct ionization. The V1 transition spectra in Fig. 5(a) are all closely similar to that of the off-resonance case, the latter being due to direct ionization alone and for which the photoelectron spectra show relaxation through the cation ground state ν_1(C≡N) stretching mode. Indeed, the off-resonance photoelectron spectrum mirrors that of the SPES spectrum in the same energy region (Figs. 2(b) and 3(a)). Thus the vibronic coupling between resonance levels involving ν_5 (C–C) excitation and the ionization continuum shows no specific peculiarities. On the other hand, Fig. 5(b), which corresponds to the V2 transition progression in the σ_g^+ ν_3 (C–C) symmetric stretch vibration does exhibit specific differences. The origin band (Band 5) photoelectron spectrum is similar to the off-resonance spectrum but excitation of the ν_3 vibration (Bands 6 and 7) give rise to modifications in vibrational peak widths and intensities in the K.E. spectra. The existence of different vibrational branching ratios indicates that there are specific differences in the processes of vibronic coupling to the ionization continuum in

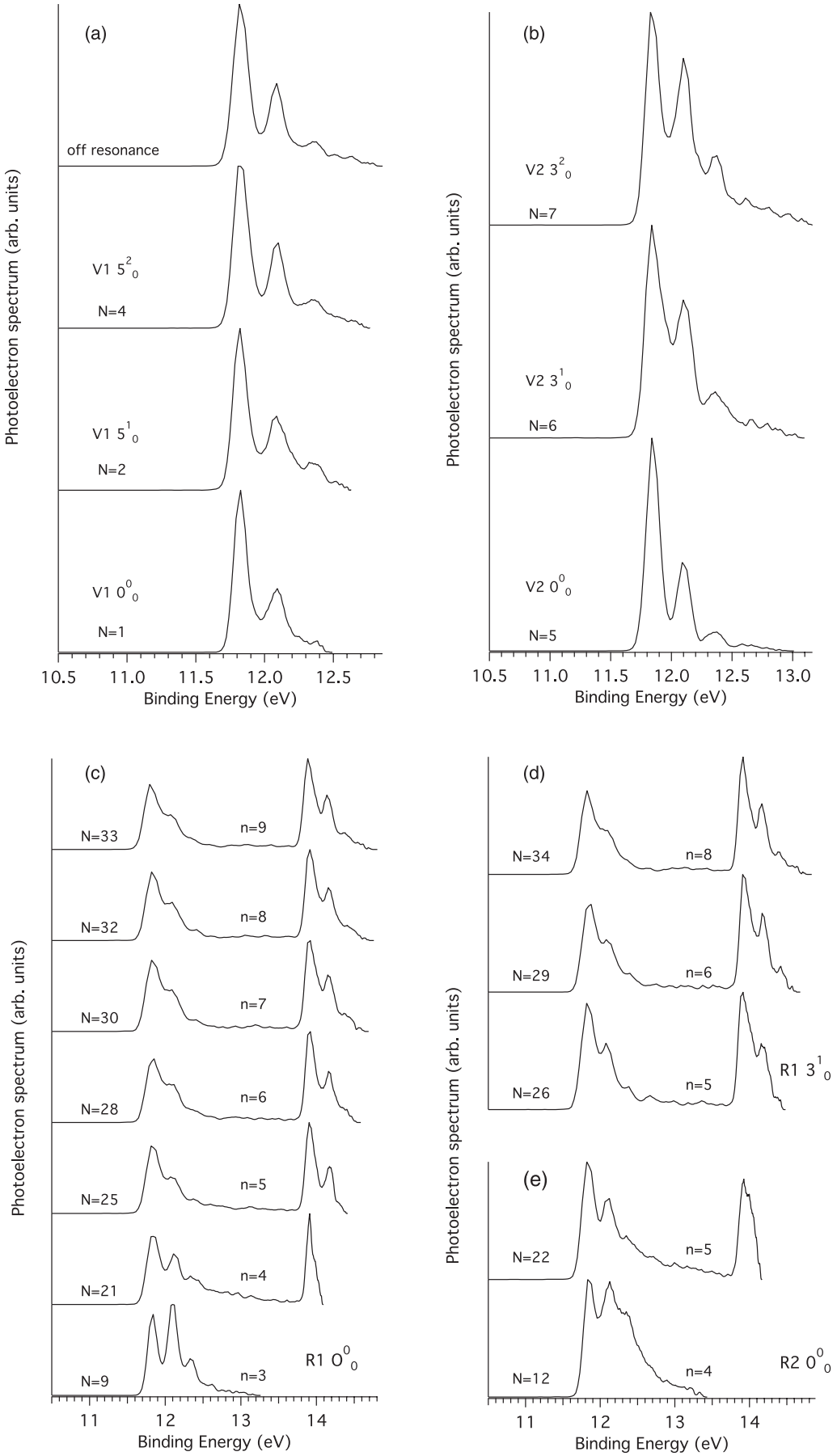

FIG. 5. (a)–(e) C_4N_2 photoelectron spectra at different fixed photon energies corresponding to the band numbers (N) referenced in Table IV. See text for description.

the two valence-shell autoionization transitions. Furthermore, the spectral behaviour of the V2 vibronic levels with increasing vibrational excitation may have its origin in an increase in vibrational redistribution in the V2 excited electronic state as the vibrational level density augments. We remark that autoionizations have been used before to probe vibrational states that are otherwise not available through direct ionization due to weak Franck-Condon overlaps.[34]

In the second energy region (Fig. 4(b)), which shows the most intense spectral features, band Nos. 9 and 12 are, respectively, assigned to the $O^0{}_0$ bands of Rydberg series R1, n = 3 and R2, n = 4 (Table IV), as discussed in Sec. IV C 3. The photoelectron spectral profile for band No. 12 (Fig. 5(d)) is somewhat broader than that for band No. 9 (Fig. 5(c)), which indicates that the autoionization rate is greater for the R2, n = 4 level.

The third region (Fig. 4(c) and Table IV) starts at 14.092 eV (band 21). It contains a number of bands that appear to be separated by an interval of ≈560 cm^{-1}, which is of the order of a ν_3 (C–C) vibrational frequency, others by apparent intervals of ≈2580 cm^{-1}, which appears too high for a dicyanoacetylene vibrational frequency. We can subdivide this region into two sub-regions: (i) 14.09–14.4 eV and (ii) E_{exc} > 14.4 eV. The first sub-region contains features (Band Nos. 21, 22, and 23), which form a progression with intervals of ≈560 cm^{-1}. In the second sub-region a similar progression in $\nu \approx 560$ cm^{-1} is observed in band Nos. 25, 26, and 27. At higher energies there are several band intervals of ≈560–600 cm^{-1}. As discussed below, many of these bands can be assigned to Rydberg series.

3. Rydberg transitions

As mentioned above, these m/z 76 TIY bands must be autoionization features. Many do not immediately appear to be Rydberg features and bear no obvious relation to some of the ionization limits of dicyanoacetylene, as shown by several attempts that we made to construct Rydberg series converging to the $A^2\Pi_g$ of the ion at 13.91 eV. The existence of three close-lying interacting ion states in the $A^2\Pi_g$ region[39,41] creates difficulties in determining Rydberg series converging to ion states in this energy region.

The bands tend to peter out in intensity at about 15 eV, where the $D^2\Pi_u$ state origin lies (Fig. 2(b) and Table IV) and we were able to assign a considerable number of bands to two Rydberg series, R1 and R2, converging to this excited ion state, with series limits corresponding to the $D^2\Pi_u$ $O^0{}_0$ state energy level (Tables III and IV). Quantum defects (δ) were determined using the standard relation $T(n) = I - R/(n - \delta)^2$, where T(n) is the energy of the spectral term whose principal quantum number is n, the Rydberg constant R = 13.606 eV and I = 14.979 eV is the energy of the $D^2\Pi_u$ $O^0{}_0$ ion state. The quantum defects are indicated in Table IV for the origin bands of each member of the Rydberg series.

The vibrational progressions in the ν_3(C–C) stretch vibration in the Rydberg series mimic those in the SPES spectra of the $D^2\Pi_u$ state (Fig. 3(c)), consistent with our Rydberg series interpretation. It is notable that this differs from the bands in the Fig. 4(a) region, which exhibit a progression in ν_5 (Table IV) and so is consistent with the bands in this region being associated with valence shell transitions, as discussed below.

The photoelectron spectra derived from Fig. 2(a) are shown in Fig. 5(c) for selected photon energies corresponding to the origin bands, i.e., the vibrationless levels, of the R1 Rydberg series n = 3–9 (Band Nos. 9, 21, 25, 28, 30, 32, and 33). The spectra are nearly identical for n ≥ 5, so that we expect the various neutral states responsible for these TIY features to be of similar geometry, consistent with a Rydberg series. The n = 4 and in particular the n = 3 photoelectron spectra show considerable differences in vibrational branching ratios with respect to the n ≥ 5 levels. This is not surprising for n = 3 levels which often show anomalous spectroscopic behaviour, sometimes due to mixing with valence states.

In Fig. 5(d) are shown photoelectron spectra for R1 Rydberg levels in which one quantum of the ν_3(C–C) stretch vibration is excited. The spectra are similar to those of the corresponding n $O^0{}_0$ levels.

Photoelectron spectra of the R2 Rydberg series are shown in Fig. 5(e) for the levels n = 4 and 5. They exhibit considerable differences in vibrational branching ratios, as well as those for corresponding n values in the R1 Rydberg series (Fig. 5(c)).

The allowed Rydberg transitions culminating in the $D^2\Pi_u$ ion state at 14.979 eV would be: one s-type and three d-type series:

$$1\pi_u{}^3 1\pi_g{}^4 3\sigma_u{}^2 4\sigma_g{}^2 1\pi_u{}^4(ns\sigma_g{}^+) \quad {}^1\Pi_u \leftarrow {}^1\Sigma_g{}^+,$$
$$1\pi_u{}^3 1\pi_g{}^4 3\sigma_u{}^2 4\sigma_g{}^2 1\pi_u{}^4(nd\sigma_g{}^+) \quad {}^1\Pi_u \leftarrow {}^1\Sigma_g{}^+,$$
$$1\pi_u{}^3 1\pi_g{}^4 3\sigma_u{}^2 4\sigma_g{}^2 1\pi_u{}^4(nd\pi_g) \quad {}^1\Sigma_u \leftarrow {}^1\Sigma_g{}^+,$$
$$1\pi_u{}^3 1\pi_g{}^4 3\sigma_u{}^2 4\sigma_g{}^2 1\pi_u{}^4(nd\delta_g) \quad {}^1\Pi_u \leftarrow {}^1\Sigma_g{}^+.$$

Our assigned R1 Rydberg series n = 3–9 have quantum defects in the range 0.08–0.18, while for the R2 Rydberg series n = 4, δ = 1.03 and n = 5, δ = 0.92 (Table IV). The R1 series most probably corresponds to states derived from *nd* electrons, giving rise to transitions such as $1\pi_u{}^3\ 1\pi_g{}^4\ 3\sigma_u{}^2\ 4\sigma_g{}^2\ 1\pi_u{}^4\ (nd\pi_g)\ {}^1\Sigma_u \leftarrow {}^1\Sigma_g{}^+$.

Concerning the R2 series we do not observe any bands for n > 5. This could be because the higher n levels of this series are predissociated, so that the corresponding ion resonance signal would be lost and also because some of bands of the higher levels could overlap with those of the R1 series. The values of the quantum defects point to an assignment of the R2 series to $ns\sigma_g{}^+$.

An alternative assignment of the two bands of the R2 series bands could be, respectively, to n = 3, δ = 0.03 and n = 4, δ = −0.08. This would also imply an nd series such as $nd\pi_g$ or $nd\delta_g$ but for these one would expect quantum defects greater than for $nd\sigma_g{}^+$. In order to check our assignment of the R2 series to $ns\sigma_g{}^+$ we calculated the probable energy of a n = 3, δ = 1, Rydberg transition. The calculated value is 11.577 eV (93 378 cm^{-1}). This is below the first ionization energy. However, Connors *et al.*[58] in a study of the VUV spectroscopy of dicyanoacetylene, observed absorption between 2000 and 1050 Å (6.2–11.8 eV), i.e., up to the first ionization energy. They used He pressure effects on the spectra, which permit distinguishing Rydberg from valence shell transitions.

The bands below 74 000 cm^{-1} (9.18 eV) were shown to be all due to valence transitions. In addition, a Rydberg series to the $X^2\Pi_u$ ground state of the dicyanoacetylene ion was identified, with a quantum defect $\delta = 0.1$ (*nd*) or 1.1 (*ns*).

Figure 5 of the publication of Connors *et al.*[58] shows the absorption spectrum of dicyanoacetylene up to the ionization limit. Examination of this spectrum revealed the existence of an unassigned absorption feature whose maximum, measured from the figure, is at 93 190 cm^{-1} (11.554 eV). This feature could therefore correspond to an n = 3 transition whose $\delta = 1.01$ and therefore to an *ns* Rydberg series. Spectral absorption studies in the 11–15 eV region could clarify the nature of the Rydberg transitions in this spectral region.

4. Valence shell transitions

Useful information pertaining to valence shell transitions relative to the TIY spectra can also be obtained from the study of Connors *et al.*[58]

Connors *et al.* carried out molecular orbital calculations of dicyanoacetylene valence shell transitions 29 300–105 100 cm^{-1} (3.63–13.03 eV), using the CNDO/2 method. In the energy region above the first IE there are calculated to be 3 intense transitions of interest, all to excited $^1\Sigma_u^+$ states:

(i) 94 900 cm^{-1} (11.77 eV, f = 0.26, $^1\Sigma_u^+$, major M.O. transitions $1\pi_u \rightarrow 2\pi_g$, $3\sigma_u \rightarrow 5\sigma_g$, $4\sigma_g \rightarrow 4\sigma_u$);
(ii) 97 300 cm^{-1} (12.06 eV, f = 0.10, $^1\Sigma_u^+$, major M.O. transitions $4\sigma_g \rightarrow 4\sigma_u$, $1\pi_g \rightarrow 3\pi_u$);
(iii) 105 100 cm^{-1} (13.03 eV, f = 1.7, $^1\Sigma_u^+$, major M.O. transitions. $4\sigma_g \rightarrow 4\sigma_u$, $1\pi_g \rightarrow 3\pi_u$).

These valence shell transitions (V) are possibly responsible for at least some of the m/z = 76 TIY bands we see in the 12.5–14 eV region and that have not been assigned to Rydberg states, in particular the bands indicated as V1 and V2 transitions.

Further work is required in order to deepen our analysis of the autoionizing features in the TIY spectra. In particular, more sophisticated calculations of the high energy valence transitions of C_4N_2 are necessary, as well as high resolution absorption spectra of dicyanoacetylene in the 11–15 eV region which would help to sort out features arising from autoionization and direct ionization and enable us to clarify and confirm the Rydberg transitions. These are planned for future studies.

D. Fragmentation of $C_4N_2^+$

Fragments originating from dissociative ionization of $C_4N_2^+$ are formed with low yields below 20 eV, typically on the order of a few percent with respect to the parent ion (cf. Fig. 1(b)). We note however that slow dissociation (i.e., slower in rate relative to the residence time of the parent in the ion acceleration regions which are 1.7 μs for $\varepsilon = 95$ V/cm, and 0.9 μs for $\varepsilon = 572$ V/cm, respectively) might lower the apparent fragment yield. In the following, we discuss the spectra of fragment ions in descending order with respect to their m/z. Note that the obtained fragment ion appearance energies (AEs) correspond to effective thermochemical energy values. As has been discussed in more detail earlier by Gaie-Levrel *et al.*[59] there are three main factors for the possible difference between the effectively measured AE and the 0 K value: (i) the limited detection sensitivity, (ii) the thermal energy stored in the parent neutral, (iii) fragmentation dynamics (possible activation barriers, formation of vibrationally excited fragments) also influence the effective AE and might lead to a substantial energy shift, ΔE, yielding a too-high AE value. The magnitude of ΔE is difficult to determine with the current experimental setup, or estimate with statistical models based on the existence of a transition state, and therefore is beyond the scope of this work. In the present molecular beam experiment, the expected low temperature (~40 K) should, however, provide a value closer to the AE_{0K} than room temperature experiments. Chupka[60] has suggested that compensatory effects between kinetic shift and temperature-determined internal energy may lead to appearance energies that reflect reasonably well their 0 K values. We consider that this is most likely to be applicable to simple bond ruptures in cases where the activation energy is small (≤1.5 eV), corresponding to a relatively low density of vibronic states in a small ion, i.e., to conditions which do not apply to dissociative photoionization processes in dicyanoacetylene.

1. $C_4N_2 + h\nu \rightarrow C_4N^+ + N$: m/z = 62

The ion yield curve of m/z = 62 is has a weak signal (not shown) but sufficient to determine the appearance energy of the C_4N^+ ion, $AE(C_4N^+) = 18.6 \pm 0.1$ eV, which is compatible with the electron impact value, $AE(C_4N^+) = 18.8 \pm 0.5$ eV of Dibeler *et al.*[56] Since $IE(C_4N_2) = 11.80 \pm 0.01$ eV, the dissociation energy $D(C_4N^+ + N) = 6.8 \pm 0.1$ eV (656 kJ/mol), assuming a simple bond rupture. This is close to the dissociation energy for the analogous channel in neutral dicyanoacetylene, $D(C_4N + N) = 6.632$ eV (640 kJ/mol) quoted by Dibeler *et al.*, indicating that ionization affects very little the CN triple bond strength. From the appearance energy of the fragment ion we determine its heat of formation as $\Delta_fH(C_4N^+) = 19.23$ eV (1855.7 kJ/mol). Dibeler *et al.* report $\Delta_fH(C_4N^+) = 19.45$ eV (1876.8 kJ/mol). Gas phase reactions of the C_4N^+ ion with a variety of molecules have been actively studied in the context of chemical evolution in astrophysical sites.[61]

2. $C_4N_2 + h\nu \rightarrow C_3N^+ + CN$: m/z = 50

The m/z = 50 ion yield curve (Fig. 6(a)) gives $AE(C_3N^+) = 18.7 \pm 0.1$ eV, which is higher than the AE = 18.4 ± 0.2 eV of the Dibeler *et al.* electron impact study.[56] We note that our value corresponds to an upper limit as has been discussed at the beginning of Sec. IV D. In addition, as can be seen from Fig. 1(e), the C_3N^+ mass peak overlaps with the broad C_4^+ mass peak so that the real onset of the C_3N^+ ion has been extracted through the deconvolution procedure described in Appendix A. Our AE must therefore be considered with caution. The dissociation energy, assuming a simple bond rupture with no energy barrier, is $D(C_3N^+ + CN) = 6.9 \pm 0.1$ eV

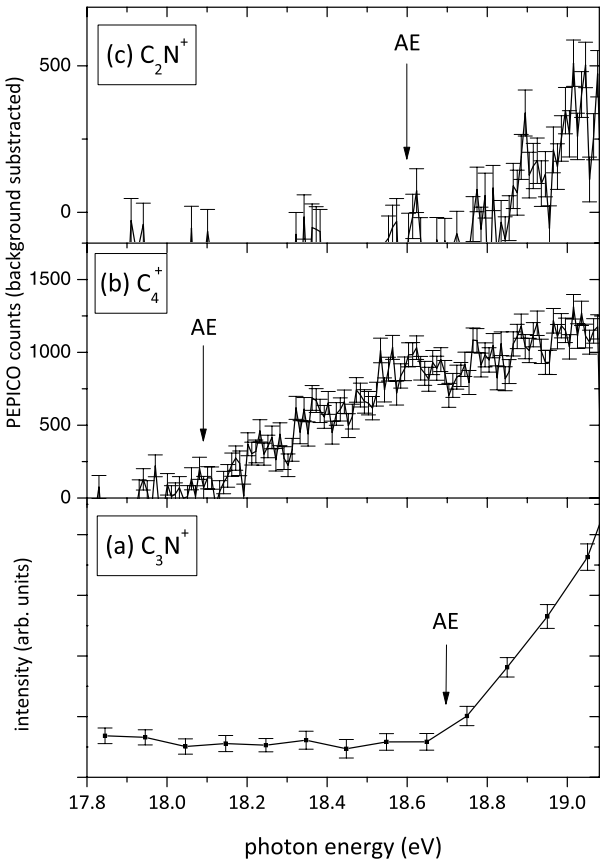

FIG. 6. (a)–(c) Photofragment ion yields for three selected ions as a function of the photon energy, recorded with an extraction field of 572 V/cm (electron $KE_{max} = 5.7$ eV). The appearance energies (AE) are marked with arrows. As discussed in Sec. IV D they correspond to effective thermochemical values. The error bars correspond to statistical noise.

(665 ± 10 kJ/mol). This is greater than the corresponding $D(C_3N + CN) = 5.34$ eV (515 ± 6 kJ/mol)[62] for neutral dicyanoacetylene, reflecting the tendency towards a cumulene carbon-carbon structure in the ion, as discussed above. From our AE for this fragment ion we calculate $\Delta_fH(C_3N^+) = 19.7 \pm 0.1$ eV (1901 ± 10 kJ/mol); Dibeler *et al.* give 20.055 eV (1935 kJ/mol);[56] Harland and Maclagan[63] and Holmes *et al.*[64] give 19.17 eV (1850 kJ/mol) for the heat of formation of a triplet state isomer of C_3N^+.

3. $C_4N_2 + h\nu \rightarrow C_4^+ + N_2$: m/z = 48

The yield curve of this ion has an experimental $AE(C_4^+) = 18.09 \pm 0.15$ eV (Fig. 6(b)). We have calculated an AE = 17.07 ± 0.70 eV (see Appendix B). Our PI MS (Fig. 1(c)) shows that C_4^+ is already present at $E_{exc} = 18$ eV, from a magnified vision of the m/z = 48 region of the $E_{exc} = 18$ eV mass spectrum. We note that an electron impact $AE(C_4^+) = 17.2 \pm 0.2$ eV is reported by Dibeler *et al.*[56] Our photon impact AE value is higher than the thermochemical and electron impact $AE(C_4^+)$ values, by about 1 and 0.9 eV, respectively. One possible explanation for this could be that the $C_4N_2 + h\nu \rightarrow C_4^+ + N_2$ reaction actually corresponds to a metastable decay which can be subject to a substantial ΔE_{kin} as discussed above. This is supported by the asymmetry of the C_4^+ mass peak seen at 18.0 and 18.5 eV (Figs. 1(c) and 1(d), resp.). We have attempted to model this asymmetric tail by numerical raytracing simulations and found values for the unimolecular fragmentation rate constant of $k = 1.5 \times 10^6$ s^{-1} at 18 eV, and 2.8×10^6 s^{-1} at 18.5 eV. We consider that these constants are reasonably high – 93% fragment detection at 18.0 eV – yielding a small kinetic shift on the effective AE.

The loss of N_2 indicates that there is a cyclic intermediate. The fact that the experimental AE is relatively close to the thermochemical value shows that the activation energies involved are small. The process of ejection of N_2 via cyclic intermediates has been explored in metastable dissociation studies of dicyanoacetylene.[65] We remark that the asymmetry of the m/z 48 ion signal, in particular at $E_{exc} = 18.5$ eV, just above the appearance threshold (Fig. 1(c)), is typical of a metastable dissociation.

We note that from our electron spectroscopy study there is no sign that a bending vibration is excited on ionization of C_4N_2. To check this point it would be worthwhile to do some higher resolution PES studies on dicyanoacetylene. In addition, some theoretical potential energy surface studies to plot out the dissociation channel $C_4^+ + N_2$ would be useful.

4. $C_4N_2 + h\nu \rightarrow C_2N^+ + C_2N$: m/z = 38

For this fragment ion the yield curve gave $AE(C_2N^+) = 18.60 \pm 0.15$ eV (Fig. 6(c)). This is higher than, but not incompatible with, the electron impact value reported by Dibeler *et al.* AE = 18.1 ± 0.4 eV,[56] given the 400 meV error limit of the latter. From $AE(C_2N^+)$ we determine a value for the dissociation energy of the central C≡C bond as 6.8 eV (656 kJ/mol), assuming a simple bond rupture with zero energy barrier. This is much greater than the CC bond energy value 5.16 eV (493 kJ/mol) quoted by Dibeler *et al.* for the $C_4N_2 \rightarrow C_2N + C_2N$ neutral dissociation process. This increase in the central CC bond energy on ionization is not consistent with the concomitant lengthening of the C–C bondlength (Table I) and it calls into question the bond energy in the neutral molecule or the possible existence of an energy barrier in the dissociative ionization process, perhaps associated with an isomerisation of $CCN^{(+)}$ to $CNC^{(+)}$. In order to determine the heat of formation of C_2N^+ from our AE value it is necessary to know the heat of formation of the other product, neutral C_2N. This is given as $\Delta_fH(C_2N) = 556$ kJ/mol,[64,66] but it is not known whether this refers to CCN or to CNC.[64] Dibeler *et al.* estimate a value $\Delta_fH(C_2N) = 514$ kJ/mol, based on various heats of formation values known in 1960, but do not specify the structure of the C_2N radical. On the assumption that it is CCN, and with the $\Delta_fH(C_2N) = 556$ kJ/mol[64,65] value, our $AE(C_2N^+) = 18.60 \pm 0.15$ eV leads to $\Delta_fH(C_2N^+) = 18.37 \pm 0.15$ eV (1772 kJ/mol). Lias *et al.* give 17.77 eV (1715 kJ/mol)[66] and Holmes *et al.* give 17.82 ± 0.21 eV (1720 ± 20 kJ/mol).[64]

5. $C_4N_2 + h\nu \rightarrow C_3^+ + CN_2$: m/z = 36

We do not observe the m/z = 36 ion. A thermochemical calculation estimate gives AE (C_3^+) = 21.0 ± 1 eV or

19.9 ± 1 eV dependent on whether the neutral product is CNN or NCN. In their electron impact study Dibeler *et al.*[56] observe AE (C_3^+) = 24.6 ± 0.5 eV, assigned to the triple product process $C_4N_2 + h\nu \rightarrow C_3^+ + CN + N$. We calculate a thermochemical AE (C_3^+) = 24.4 ± 1.0 eV for this process, in excellent agreement with the Dibeler *et al.* appearance energy for this fragment ion.

6. $C_4N_2 + h\nu \rightarrow N_2^+ + C_4$: m/z = 28

We observe the N_2^+ ion at m/z = 28 but at its onset energy, 15.58 eV, it is obviously from an air impurity. It is not possible to determine whether the m/z = 28 includes a contribution from the C_4 loss channel. A thermochemical calculation predicts AE(N_2^+) = 20.12 ± 0.35 eV as the lowest possible appearance energy for this channel. There is no electron impact report for this channel.[56] The m/z = 28 ion is not present in the electron impact mass spectra of dicyanoacetylene presented in the NIST collection.[57]

7. $C_4N_2 + h\nu \rightarrow CN^+ + C_3N$: m/z = 26

Dibeler *et al.* report AE(CN^+) = 19.2 ± 0.3 eV, intensity 5.3%, in their electron impact study.[56] This ion is not present in our photoionization mass spectra at E_{exc} = 20 and 25 eV. We calculate a thermochemical AE(CN^+) = 16.27 eV for this dissociative ionization process, which is much below the Dibeler *et al.* AE value. This is probably indicative of an energy barrier of the order of 3 eV. We note that for the triple product channels $C_4N_2 + h\nu \rightarrow$ (i) $CN^+ + C_3 + N$ and (ii) $CN^+ + C_2 + CN$, we calculate thermochemical AE values of, respectively, (i) 26.17 eV and (ii) 25.732 eV. These are much higher than the electron impact AE(CN^+) = 19.2 ± 0.3 eV, thus adding justification for the binary product channel with a ≈ 3 eV energy barrier.

8. $C_4N_2 + h\nu \rightarrow C_2^+ + C_2N_2$: m/z = 24

Dibeler *et al.* report an electron impact AE(C_2^+) = 18.5 ± 0.3 eV.[56] We observe a weak signal at this mass at E_{exc} = 20, 19.5, and 19 eV (not shown) but not at 18.5 eV, nor at 25 eV. We can therefore give an experimental AE(C_2^+) = 18.75 ± 0.25 eV. The thermochemical calculation value is AE(C_2^+) = 18.37 eV, in agreement with the Dibeler *et al.* and our observations.

9. $C_4N_2 + h\nu \rightarrow N^+ + C_3 + CN$: m/z = 14

In their electron impact study Dibeler *et al.* observe AE(N^+) = 26.0 ± 1.0 eV and tentatively propose the triple product channel.[56] In our photoionization study we did not observe this ion up to and including E_{exc} = 25 eV. We calculate a thermochemical value AE(N^+) = 27.08 eV for this triple product process, which is compatible with the observed appearance energy although it would correspond to an unlikely zero energy barrier process. We also made a thermochemical calculation of the N^+ appearance energy for the binary product process $C_4N_2 + h\nu \rightarrow N^+ + C_4N$. The value obtained, AE(N^+) = 20.66 eV is about 6 eV below the electron impact AE, which is rather large. We suggest that the AE(N^+) = 26.0 ± 1.0 eV observed by Dibeler *et al.* is due to an unacknowledged nitrogen impurity (no ion signal at m/z = 28 (N_2^+) was reported in their study). The process $N_2 + h\nu \rightarrow N^+ + N$ has an appearance energy AE(N^+) = 24.34 eV.[57]

10. $C_4N_2 + h\nu \rightarrow C^+ + C_3N_2$: m/z = 12

Dibeler *et al.* observed AE(C^+) = 24 ± 1 eV in their electron impact study.[56] It was not observed in our photon impact mass spectra at E_{exc} = 25 eV. Dibeler *et al.* tentatively propose the binary product process $C_4N_2 + h\nu \rightarrow C^+ + C_3N_2$. A thermochemical calculation for this process is not possible since a value of $\Delta_fH(C_3N_2)$ is lacking. We calculated the thermochemical value AE(C^+) = 21.65 eV for a triple product process $C_4N_2 + h\nu \rightarrow C^+ + C_3 + N_2$, which is not incompatible with the electron impact AE(C^+) = 24 ± 1 eV.

V. CONCLUDING REMARKS

Dicyanoacetylene and its ions are important species whose presence in astrophysical sites is expected or observed. In particular these species play a role in the atmosphere of Titan where they are subject to charged particle and photon irradiation. The effects of VUV radiation on dicyanoacetylene were studied using synchrotron radiation combined with electron/ion coincidence techniques over the excitation range 8–25 eV. A detailed analysis of the SPES spectrum in the 11.5–15.5 eV excitation energy region was carried out. The $X^2\Pi_u$ ground state of the cation shows an onset at IE_{ad} = 11.80 eV in the TIY spectrum, in reasonable agreement with previous PES values, and exhibits vibrational components in the SPES spectra in the 11.8–13.8 eV region which involve the ν_1 (N≡C), ν_2 (C≡C), ν_3 (C–C) and ν_7 (bend) frequencies. Analysis of SPES features in the 13.8–14.4 eV spectral region provides new aspects and new assignments of vibrational components to the excited quasi-degenerate $A^2\Pi_g$, $B^2\Sigma_g^+$ states, whose origin band is at 13.907 eV, as well as the $C^2\Sigma_u^+$ state at 14.178 eV. SPES bands in the 14.9–15.5 eV region contain the origin band of the $D^2\Pi_u$ state of the cation, observed at 14.979 ± 0.10 eV, and vibrational components mainly in ν_3 (C–C).

The total ionization cross-section has been measured in an absolute scale over the 11.5–15.5 eV photon energy range and exhibits structured autoionization features in the 12.4–15 eV region. They were assigned to vibrational components of valence shell transitions and to members of two previously unknown Rydberg series, converging to the O^0_0 level of the $D^2\Pi_u$ state of $C_4N_2^+$. Some aspects of the autoionization processes were monitored via photoelectron kinetic energy spectra measured at a number of specific photon excitation energies.

The appearance energies of the fragment ions C_4N^+, C_3N^+, C_4^+, and C_2N^+ were measured and their heats of formation were determined and compared with existing literature values. Thermochemical calculations of the appearance

potentials of these and other weaker ions were used to infer aspects of dissociative ionization pathways. Particular problems of calculating thermochemical appearance energies arise in the case of the C_4^+ and C_2N^+ ions and are discussed in detail.

Theoretical calculations are required in order to refine our spectroscopic results involving valence shell and Rydberg transitions, as well as some of the observed dissociative ionization processes. We hope that the present study will encourage useful computational activity on these questions.

Concerning astrophysical implications of our results, we remark that the dicyanoacetylene cation is very stable under VUV irradiation. The first dissociative ionization process occurs at about 18 eV, i.e., at over 6 eV above the ionization energy, and about 4.4 eV above the astrophysical H I energy upper limit, 13.6 eV. Thus if C_4N_2 is formed in HI regions of the interstellar medium (ISM) it should have no tendency to undergo dissociative ionization in these regions. Indeed, the partial cross-sections for the dissociative photoionization processes are at most only a few percent of that of the parent ion up to 19 eV. We remark also that using the rule of thumb[67] concerning the quasi-linearity of the ionization quantum yield Φ_i as a function of excitation energy in a range up to ≈9.2 eV above the ionization energy, where Φ_i becomes ≈100%, we can determine that the ionization quantum yield of dicyanoacetylene will be about 67% at 18 eV, so that about 33% of the photon excitation will be to superexcited states at this energy. These superexcited states can undergo a variety of relaxation processes, including autoionization, dissociative autoionization and neutral dissociation. They can also play a role as reaction intermediates or collision complexes in electron-ion recombination, electron attachment and Penning ionization.[68]

At $E_{exc} = 15$ eV, below the dissociative ionization threshold, the total ionization cross-section is 6×10^{-18} cm^2 (Fig. 2). At this photon excitation energy we can estimate from the rule of thumb that the ionization quantum yield is about 35%, so that we can predict an absorption cross-section of 17.1×10^{-18} cm^2 at 15 eV. We plan to carry out VUV absorption measurements on dicyanoacetylene in the 15 eV region at the earliest possible opportunity in order to verify these prognostics.

One striking result of our study concerns the relative photoionization cross-sections of diacetylene and dicyanoacetylene. At a comparable 4 eV energy above the ionization energy of diacetylene, and equally below the initial dissociative ionization energy of C_4H_2, its ionization cross section is $\approx 15 \times 10^{-18}$ cm^2,[3] i.e., about 2.5 times the corresponding 6×10^{-18} cm^2 value for dicyanoacetylene. The cross-sections of the strong Rydberg features in the corresponding TIY curves are also about 2.5 times greater in C_4H_2[3] than in C_4N_2. Furthermore, it is striking that for the similarly related species acetylene and cyanogen, the calculated partial channel (ion ground state) photoionization cross-section for C_2H_2[69] is also 2–2.5 times greater than for C_2N_2[70] up to 40 eV. Since the absorption cross-sections in the 15 eV region are roughly similar for acetylene[71–73] and cyanogen,[74] the difference in photoionization cross-sections in this energy region must be related to the ionization quantum yield which, according to the rule of thumb (which will only be a coarse-grained relation for these small species, neglecting shape resonances), will be greater by about a factor of 2.2 for acetylene with respect to cyanogen at 15 eV. Absorption studies of diacetylene and dicyanoacetylene in the 15 eV region are required in order to elucidate their relative photoionization cross-section behaviours.

ACKNOWLEDGMENTS

We are indebted to the general staff of SOLEIL for running the synchrotron radiation facility, and in particular to J.-F. Gil, for technical help on the DESIRS beamline. We thank the French National program Physique et Chimie du Milieu Interstellaire for financial support.

APPENDIX A: EXTRACTION OF C_3N^+ ION YIELD CURVE

As discussed in Sec. IV B 2, the asymmetric tail due to the metastability of the C_4^+ peak overlaps with the adjacent C_3N^+. Therefore, a deconvolution procedure has been applied to extract the true ion yield of C_3N^+. The C_4^+ peak has been modelled with a Gaussian function convoluted with an exponential decay, while only a Gaussian has been used for the C_3N^+ peak. The function coefficients are then extracted *via* weighted least-squares fitting of this model to the experimental TOF, and the C_3N^+ ion yield obtained as the surface under its Gaussian function. An example of such a fit is shown in Fig. 7. Due to the low fragment signals, the fit has not been performed at each scan photon energy, so that each data point in Fig. 6(a) corresponds to the integration of ten scan points. The TOF temporal resolution had to be also decreased by ten to further increase the statistics.

APPENDIX B: $C_4N_2^+$: THERMOCHEMICAL CALCULATED APPEARANCE ENERGY OF C_4^+

We seek to calculate a thermochemical value for the appearance energy AE(C_4^+) in the dissociative ionization process $C_4N_2 + h\nu \rightarrow C_4^+ + N_2$. For this we need to determine the heat of formation $\Delta_fH(C_4^+) \rightarrow \Delta_fH(C_4) + IE(C_4)$. It is known that the C_4 radical can exist in several different

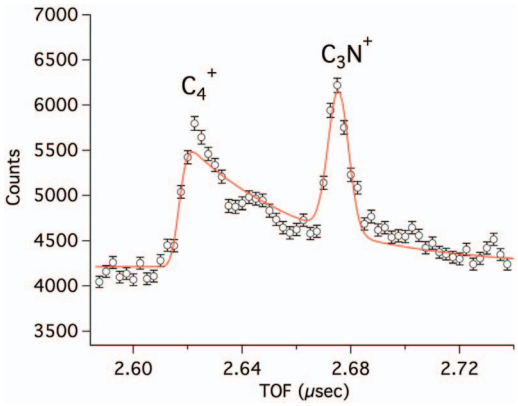

FIG. 7. Experimental (black circles) and model (red line) ion TOF obtained at $h\nu = 19.05$ eV with an extraction field of 572 V/cm, showing the overlap between the C_4^+ and C_3N^+ masses. See text for details on the model.

geometrical forms.[75,76] Two isomers are known experimentally, a linear form and a rhombic form, of similar stabilities, and at least two other higher-lying isomers could exist.[77] The calculations of Kosimov *et al.*[78] indeed showed the possible existence of five different geometrical structures. From an examination of the results of the various calculations by the various authors quoted in Ref. 78, we conclude as most probable that the linear and rhombic forms of C_4 are quasi-isoenergetic, with the linear form being marginally more stable. The C_4^+ ion is thus also capable of existing in several geometrical forms.[79]

A heat of formation value $\Delta_f H\ (C_4) = 971 \pm 33$ kJ/mol is given by Lias *et al.*[65] but whether this refers to the linear or the rhombic structure is not specified. The ionization energy value $IE(C_4) = 12.54 \pm 0.35$ eV[57] was determined by Ramanathan *et al.*[80] by charge transfer bracketing. An earlier electron impact measurement of the ionization of carbon vapour gave $IE(C_4) = 12.6$ eV.[81] However, the results of some theoretical calculations on various C_4 isomers suggest 1–2 eV lower values of the ionization energy.[79] From the NIST thermochemistry data and the reported experimental $IE(C_4) = 12.54 \pm 0.35$ eV, we calculate that the appearance energy of C_4^+ would be 17.07 ± 0.35 eV in the case of the dissociative photoionization of C_4N_2, which is compatible with our experimental value, $AE(C_4^+) = 18.09 \pm 0.15$ eV. The structures of neutral and cationic C_4 involved in these experiments and in the thermochemical calculations on this dicyanoacetylene dissociative ionization channel remain to be determined more precisely.

[1] C. Moreau and J. C. Bongrand, Ann. Chim. (Paris) **14**, 5 (1920).
[2] C. D. Weis, J. Org. Chem. **28**, 74 (1963).
[3] M. Schwell, Y. Benilan, N. Fray, M.-C. Gazeau, Et. Es-Sebbar, F. Gaie-Levrel, N. Champion, and S. Leach, Mol. Phys. **110**, 2843 (2012).
[4] R. Kołos, J. Chem. Phys. **117**, 2063 (2002).
[5] L. W. Avery, N. W. Broten, J. M. MacLeod, T. Oka, and H. W. Kroto, Astrophys. J. **205**, L173 (1976).
[6] M. B. Bell, P. A. Feldman, M. J. Travers, M. C. McCarthy, C. A. Gottlieb, and P. Thaddeus, Astrophys. J. **483**, L61 (1997).
[7] H. Suzuki, S. Yamamoto, M. Ohishi, N. Kaifu, S.-I. Ishikawa, Y. Hirahara, and S. Takano, Astrophys. J. **392**, 551 (1992).
[8] J. Cernicharo, A. M. Heras, A. G. G. M. Tielens, J. R. Pardo, F. Herpin, M. Guélin, and L. B. F. M. Waters, Astrophys. J. **546**, L123 (2001).
[9] J. R. Pardo, J. Cernicharo, and J. R. Goicoechea, Astrophys. J. **628**, 275 (2005).
[10] R. K. Khanna, M. A. Perera-Jarmer, and M. J. Ospina, Spectrochim. Acta A **43**, 421 (1987).
[11] F. Winther, ASP Conf. Ser. **81**, 327 (1995).
[12] T. Motylewski, H. Linnartz, O. Vaizert, J. P. Maier, G. A. Galazutdinov, F. A. Musaev, J. Krełowski, G. A. H. Walker, and D. A. Bohlender, Astrophys. J. **531**, 312 (2000).
[13] E. H. Wilson and S. K. Atreya, J. Geophys. Res. E **109**, E06002, doi:10.1029/2003JE002181 (2004).
[14] R. E. Samuelson, L. A. Mayo, M. A. Knuckles, and R. J. Khanna, Planet. Space Sci. **45**, 941 (1997).
[15] V. A. Krasnopolsky, Icarus **201**, 226 (2009).
[16] Y. L. Yung, Icarus **72**, 468 (1987).
[17] S. Petrie and Y. Osamura, J. Phys. Chem. A **108**, 3623 (2004).
[18] J. B. Halpern, G. E. Miller, and H. Okabe, Chem. Phys. Lett. **155**, 347 (1989).
[19] P. P. Lavas, A. Coustenis, and I. M. Vardavas, Planet. Space Sci. **56**, 27 (2008).
[20] P. P. Lavas, A. Coustenis, and I. M. Vardavas, Planet. Space Sci. **56**, 67 (2008).
[21] V. Vuitton, R. V. Yelle, and M. J. McEwan, Icarus **191**, 722 (2007).
[22] K. Graupner, T. A. Field, and G. C. Saunders, Astrophys. J. **685**, L95 (2008).
[23] F. Sebastianelli and F. A. Gianturco, Eur. Phys. J. D **59**, 389 (2010).
[24] T. J. Millar, C. Walsh, M. A. Cordiner, Ní Chuimín, and E. Herbst, Astrophys. J. **662**, L87 (2007).
[25] A. J. Coates, F. J. Crary, G. R. Lewis, D. T. Young, J. H. Waite, Jr., and E. C. Sitter, Jr., Geophys. Res. Lett. **34**, L22103, doi:10.1029/2007GL030978 (2007).
[26] V. Vuitton, P. Lavvas, R. V. Yelle, M. Galland, A. Wellbrock, G. R. Lewis, A. J. Coates, and J.-E. Wahlund, Planet. Space Sci. **57**, 1558 (2009).
[27] W. C. Maguire, Bull. Am. Astron. Soc. **27**, 1089 (1995).
[28] C. Moureu and J. C. Bongrand, Ann. Chim. (Paris) **14**, 47 (1920).
[29] F. A. Miller and D. H. Lemmon, Spectrochim. Acta, Part A **23**, 1415 (1967).
[30] L. Nahon, N. de Oliviera, G. A. Garcia, J.-F. Gil, B. Pilette, O. Marcouillé, B. Lagarde, and F. Polack, J. Synchrotron Radiat. **19**, 508 (2012).
[31] B. Mercier, M. Compin, C. Prevost, G. Bellec, R. Thissen, O. Dutuit, and L. Nahon, J. Vac. Sci. Technol. A **18**, 2533 (2000).
[32] G. A. Garcia, H. Soldi-Lose, and L. Nahon, Rev. Sci. Instrum. **80**, 023102 (2009).
[33] J. C. Poully, J. P. Schermann, N. Nieuwjaer, F. Lecomte, G. Grégoire, C. Desfrançois, G. A. Garcia, L. Nahon, D. Nandi, L. Poisson, and M. Hochlaf, Phys. Chem. Chem. Phys. **12**, 3566 (2010).
[34] M. Briant, L. Poisson, M. Hochlaf, P. de Pujo, M.-A. Gaveau, and B. Soep, Phys. Rev. Lett. **109**, 193401 (2012).
[35] T. A. Cool, J. Wuang, K. Nakajima, C. A. Taatjes, and A. McIlroy, Int. J. Mass Spectrom. **247**, 18 (2005).
[36] K. Kameta, N. Kouchi, M. Ukai, and Y. Hatano, J. Electron Spectrosc. Relat. Phenom. **123**, 225 (2002).
[37] G. Bieri, E. Heilbronner, V. Hornung, E. Kloster-Jensen, J. P. Maier, F. Thommen, and W. Von Neissen, Chem. Phys. **36**, 1 (1979).
[38] L. Åsbrink, W. Von Neissen, and G. Bieri, J. Electron Spectrosc. Relat. Phenom. **21**, 93 (1980).
[39] J. P. Maier, L. Misev, and F. Thommen, J. Phys. Chem. **86**, 514 (1982).
[40] Z. Cao and S. D. Peyerimhoff, J. Phys. Chem. A **105**, 627 (2001).
[41] W. E. Sinclair, D. Pfluger, and J. P. Maier, J. Chem. Phys. **111**, 9600 (1999).
[42] K. W. Brown, J. W. Nibler, K. Hedberg, and L. Hedberg, J. Phys. Chem. **93**, 5679 (1989).
[43] G. Fischer and I. G. Ross, J. Phys. Chem. **107**, 10631 (2003).
[44] J. O. Jensen, J. Mol. Struct.: THEOCHEM **678**, 233 (2004).
[45] S. Lee, J. Phys. Chem. **100**, 13959 (1996).
[46] J. M. Lee and L. Adamowicz, Spectrochim. Acta, Part A **57**, 897 (2001).
[47] Y. Zhao, J. Guo, and J. Zhang, Theor. Chem. Acc. **129**, 793 (2011).
[48] F. Winther and M. Schönhoff, J. Mol. Spectrosc. **186**, 54 (1997).
[49] J. P. Maier, O. Marthaler, and F. Thommen, Chem. Phys. Lett. **60**, 193 (1979).
[50] J. Agreiter, A. M. Smith, M. Härtle, and V. E. Bondybey, Chem. Phys. Lett. **225**, 87 (1994).
[51] C. Baker and D. W. Turner, Proc. R. Soc. London, Ser. A **308**, 19 (1968).
[52] A. M. Smith-Gicklhorn, M. Lorenz, R. Kołos, and V. E. Bondybey, J. Chem. Phys. **115**, 7534 (2001).
[53] R. Rankovic, S. Jerosimic, and M. Peric, J. Chem. Phys. **135**, 024314 (2011).
[54] G. A. Garcia, L. Nahon, and I. Powis, Rev. Sci. Instrum. **75**, 4989 (2004).
[55] R. Nagarajan and J. P. Maier, Int. Rev. Phys. Chem. **29**, 521 (2010).
[56] V. H. Dibeler, R. M. Reese, and J. L. Franklin, J. Am. Chem. Soc. **83**, 1813 (1961).
[57] NIST Chemistry Webbook, National Institute of Standards and Technology Reference Database, June 2005, see http://webbook.nist.gov (current 2009).
[58] R. E. Connors, J. L. Roebber, and K. Weiss, J. Chem. Phys. **60**, 5011 (1974).
[59] F. Gaie-Levrel, C. Gutlé, H.-W. Jochims, E. Rühl, and M. Schwell, J. Phys. Chem. A **112**, 5138 (2008).
[60] W. A. Chupka, J. Chem. Phys. **30**, 191 (1959).
[61] D. K. Bohme, S. Wlodek, and A. B. Raksit, Can. J. Chem. **65**, 1563 (1987).
[62] J. B. Halpern, L. Petway, R. Lu, W. M. Jackson, V. R. McCrary, and W. Nottingham, J. Phys. Chem. **94**, 1869 (1990).
[63] P. W. Harland and R. G. A. R. Maclagan, J. Chem. Soc., Faraday Trans. 2 **83**, 2133 (1987).
[64] J. L. Holmes, C. Aubry, and P. M. Mayer, *Assigning Structures to Ions in Mass Spectrometry* (CRC Press, Boca Raton, 2007).
[65] D. Sülzle, K. Seemeyer, H. Schwarz, B. Witulski, and H. Hopf, Int. J. Mass Spectrom. Ion Process. **105**, R1 (1991).

[66]S. G. Lias, J. E. Bartmess, J. F. Libman, J. L. Holmes, R. D. Levin, and W. G. Mallard, J. Phys. Chem. Ref. Data **17**(Suppl. 1) (1988).
[67]H.-W. Jochims, H. Baumgärtel, and S. Leach, Astron. Astrophys. **314**, 1003 (1996).
[68]Y. Hatano, Phys. Rep. **313**, 109 (1999).
[69]D. Lynch, M.-T. Lee, R. R. Lucchese, and V. McKoy, J. Chem. Phys. **80**, 1907 (1984).
[70]D. Lynch, S. N. Dixit, and V. McKoy, J. Chem. Phys. **84**, 5504 (1986).
[71]C. Y. R. Wu and D. L. Judge, J. Chem. Phys. **82**, 4495 (1985).
[72]J. C. Han, C. Ye, M. Suto, and L. C. Lee, J. Chem. Phys. **90**, 4000 (1989).
[73]M. Ukai, K. Kameta, R. Chiba, K. Nagano, N. Kouchi, K. Shinsaka, Y. Hatano, H. Umemoto, Y. Ito, and K. Tanaka, J. Chem. Phys. **95**, 4142 (1991).
[74]J. A. Nuth and S. Glicker, J. Quant. Spectrosc. Radiat. Transf. **28**, 223 (1982).
[75]M. Algranati, H. Feldman, D. Kella, E. Malkin, E. Miklazky, R. Naaman, Z. Vager, and J. Zajfman, J. Chem. Phys. **90**, 4617 (1989).
[76]D. Kella, D. Zajfman, O. Heber, D. Majer, H. Feldman, Z. Vager, and R. Naaman, Z. Phys. D: At., Mol. Clusters **26**, 340 (1993).
[77]H. Massó, M. L. Senent, P. Rosmus, and M. Hochlaf, J. Chem. Phys. **124**, 234304 (2006).
[78]D. P. Kosimov, A. A. Dzhurakhalov, and F. M. Peeters, Phys. Rev. B **78**, 235433 (2008).
[79]M. Hochlaf, C. Nicolas, and L. Poisson, J. Chem. Phys. **127**, 014310 (2007).
[80]R. Ramanathan, J. A. Zimmerman, and J. R. Eyler, J. Chem. Phys. **98**, 7838 (1993).
[81]J. Drowart, R. P. Burns, G. DeMaria, and M. G. Inghram, J. Chem. Phys. **31**, 1131 (1959).